Fuel 234 (2018) 1431–1451

Contents lists available at ScienceDirect

Fuel

journal homepage: www.elsevier.com/locate/fuel

Full Length Article

# Improving carbon efficiency and profitability of the biomass to liquid process with hydrogen from renewable power

M. Hillestad[a,*], M. Ostadi[a], G.d. Alamo Serrano[b], E. Rytter[a], B. Austbø[c], J.G. Pharoah[d], O.S. Burheim[e]

[a] Department of Chemical Engineering, Norwegian University of Science and Technology, NO-7491 Trondheim, Norway
[b] SINTEF Energy Research, N-7465 Trondheim, Norway
[c] Department Mechanical and Industrial Engineering, Norwegian University of Science and Technology (NTNU), Trondheim, Norway
[d] Department of Mechanical and Materials Engineering, Queens University, Kingston, Canada
[e] Department Energy and Process Engineering, Norwegian University of Science and Technology, Trondheim, Norway

## GRAPHICAL ABSTRACT

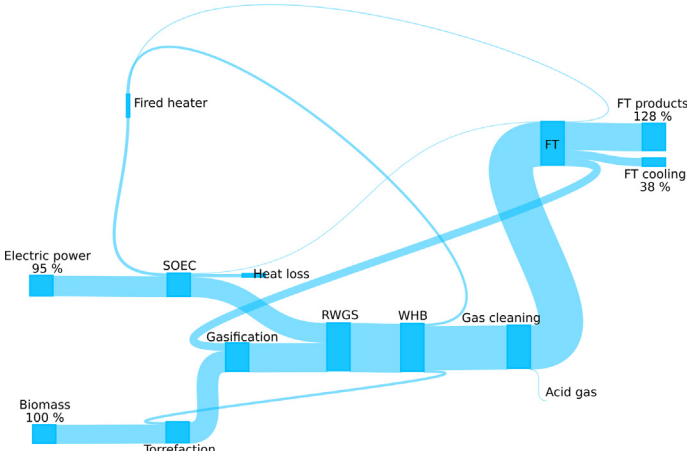


## ARTICLE INFO

*Keywords:*
Power and biomass to liquid
Reversed water gas shift
Fischer-Tropsch
Entrained flow gasification
Solid oxide electrolysis
Acid gas removal

## ABSTRACT

A process where power and biomass are converted to Fischer-Tropsch liquid fuels (PBtL) is compared to a conventional Biomass-to-Liquid (BtL) process concept. Based on detailed process models, it is demonstrated that the carbon efficiency of a conventional Biomass to Liquid process can be increased from 38 to more than 90% by adding hydrogen from renewable energy sources. This means that the amount of fuel can be increased by a factor of 2.4 with the same amount of biomass. Electrical power is applied to split water/steam at high temperature over solid oxide electrolysis cells (SOEC). This technology is selected because part of the required energy can be replaced by available heat. The required electrical power for the extra production is estimated to be 11.6 kWh per liter syncrude ($C_{5+}$). By operating the SOEC iso-thermally close to 850 °C the electric energy may be reduced to 9.5 kWh per liter, which is close to the energy density of jet fuel. A techno-economic analysis is performed where the total investments and operating costs are compared for the BtL and PBtL. With an electrical power price of 0.05 $/kWh and with SOEC investment cost of the 1000 $/kW(el), the levelized cost of producing

* Corresponding author.
*E-mail addresses:* magne.hillestad@ntnu.no (M. Hillestad), mohammad.ostadi@ntnu.no (M. Ostadi), Gonzalo.Alamo@sintef.no (G.d. Alamo Serrano), erling.rytter@ntnu.no (E. Rytter), bjorn.austbo@ntnu.no (B. Austbø), pharoah@queensu.ca (J.G. Pharoah), burheim@ntnu.no (O.S. Burheim).

https://doi.org/10.1016/j.fuel.2018.08.004
Received 19 March 2018; Received in revised form 7 June 2018; Accepted 1 August 2018

advanced biofuel with the PBtL concept is 1.7 $/liter, which is approximately 30% lower than for the conventional BtL. Converting excess renewable electric power to advanced biofuel in a PBtL plant is a sensible way of storing energy as a fuel with a relatively high energy density.

**Nomenclature**

*Acronyms*

| | |
|---|---|
| ASU | Air separation unit |
| BtL | A process for converting Biomass to Liquids via the Fischer-Tropsch synthesis |
| CSTR | Completely stirred tank reactor |
| EFG | Entrained Flow Gasifier |
| FT | Fischer-Tropsch |
| FTS | Fischer-Tropsch Synthesis |
| LHV | Lower Heating Value |
| PBtL | A process for converting Power and Biomass to Liquids via the Fischer-Tropsch synthesis |
| RWGS | Reversed Water Gas Shift reactor |
| SOEC | Solid Oxide Electrolysis Cells |
| WGS | Water Gas Shift reactor |
| WHB | Waste Heat Boiler |

*Symbols*

| | |
|---|---|
| $\alpha_1$ | The chain growth (polymerization probability) of paraffin production |
| $\alpha_2$ | The chain growth of olefin production |
| $\delta_{elt}$ | Electrolyte thickness [m] |
| $\dot{n}$ | Molar flow rate of steam to the SOEC [kmol/h] |
| $\nu_{i,j}$ | Stoichiometric coefficient of reaction $i$ and component $j$ |
| $\sigma_{elt}$ | Electrical conductivity of cell [S/m$^2$] |
| $I$ | Electrical current through the cell [A] |
| $r_i$ | Reaction rate of reaction $i$ = 1, 2, 3, 4 for reactions defined in Eqs. (6)–(9) |
| $R_{elt}$ | Ohmic resistance over the cell [Ω] |
| $T_{TN}$ | Thermal neutral temperature [K] |
| $U_1$ | Stoichiometric consumption ratio $H_2$/CO of paraffin production. |
| $U_2$ | Stoichiometric consumption ratio $H_2$/CO of olefin production. |
| | Electrical work supplied to the SOEC [MW] |
| $X$ | The conversion of steam in the SOEC |

## 1. Introduction

As the first industrial sector, the aviation industry has committed to a set of ambitious high-level goals to reduce its carbon emissions at a global level. The International Air Transport Association (IATA) has taken an initiative; CORSIA [1], where the aviation industry is committed to technology, operational and infrastructure advances to continue to reduce the sector's carbon emissions. One of the four-pillar strategy to reach their goals is improved technology, which includes the deployment of sustainable alternative fuels. For the aviation industry there are few realistic alternatives to kerosene and jet fuel, mainly because a fuel with high energy density is required. If the industry is to reduce their carbon emission, advanced biofuel based on Fischer-Tropsch synthesis and renewable power is a realistic option. This study evaluates a process concept that reduces the $CO_2$ release from conventional biomass to liquid plants and has the potential for reducing the price of advanced biofuel [1] for the aviation industry.

A process where woody biomass is converted to liquid hydrocarbons via the Fischer-Tropsch (FT) synthesis is often referred to as a biomass to liquid process, or simply BtL. Even though BtL can include other technologies, the FT route is considered here. In the Fischer-Tropsch synthesis, hydrogen and CO react on a solid catalyst to form a distribution of hydrocarbons and water. The stoichiometric consumption ratio $H_2$/CO is slightly higher than two. However, when biomass is gasified, the product gas, i.e. the synthesis gas or syngas, has a $H_2$/CO ratio of less than one. In order to increase the ratio to a level that is suitable for Fischer-Tropsch synthesis, the conventional way of thinking is to add steam to the syngas so that CO is shifted to $CO_2$ and $H_2$ in a water gas shift reactor (WGS) at a lowered temperature. The problem with this is that more than half of the biomass carbon ends up as $CO_2$ and not in the product.

Another way of seeing the limitation is by looking at the energy content of dry biomass compared to the product FT diesel; the lower heating values are ca 19 and 42 MJ/kg, respectively. Without adding extra energy to the process, a large carbon loss is inevitable. The limitation is connected to the conservation of energy. If all the biomass carbon ends up in the fuel, the energy conservation principle will be violated without adding extra energy; more energy out than energy in. Therefore some carbon has to go out as $CO_2$ with LHV = 0 without adding extra energy.

Rytter et al. [2] reported carbon efficiencies of 24, 33 and 38%, respectively, for the following combinations of biomass pre-treatment and gasification technologies; chipping and circulating fluidized-bed, torrefaction and entrained-flow, and pyrolysis and entrained-flow. Corresponding energy efficiencies were reported as 27, 27 and 33%, respectively.

An alternative to shifting the syngas to increase the $H_2$/CO ratio, is to add external energy as hydrogen to the process. There are studies in the literature where this is suggested, and a few process concepts are patented. Agrawal et al. [3] proposed a hybrid hydrogen-carbon process for production of liquid hydrocarbon fuels where the biomass is seen as the carbon source and hydrogen as an energy carrier supplied from carbon-free energy source. Bernical et al. [4] suggested to keep the WGS reactor on part of the syngas to increase the $H_2$/CO ratio somewhat, in addition to use hydrogen from high temperature steam electrolysis to adjust the $H_2$/CO ratio to the required ratio to the FT synthesis.

In another study, Hannula [5] investigated gasification of woody biomass to produce fuels like gasoline and methane with the addition of external hydrogen. Compared to reference plants, his calculations indicate that by adding external hydrogen, the fuel output can be increased by a factor of 2.6 and 3.1 for gasoline and methane, respectively. The cost estimates presented by Hannula indicate that a levelized cost of hydrogen below 2.2–2.8 Euro/kg will make the process competitive to the reference process.

In a recent article, Dietrich et al. [6] presented three process concepts where hydrogen and oxygen from water electrolysis are utilized

[1] Advanced biofuel technology are technologies which are still in the research & development, pilot or demonstration phase, commonly referred to as second- and third-generation

and where hydrogen is applied in a reversed water gas shift reactor to shift $CO_2$ to CO in order to increase the carbon efficiency. They compared three different process concepts; (1) the conventional BtL without any addition of hydrogen, (2) using renewable power to produce hydrogen combined with BtL and (3) to convert $CO_2$ from combustion to produce CO and further to Fischer-Tropsch products.

Here, the process concept with adding renewable hydrogen to a BtL is further developed and improved. In addition, a detailed model of the process is developed. Extra energy is added to the BtL as hydrogen produced from renewable power, hence PBtL. Hydrogen is produced through high temperature steam electrolysis in a solid oxide electrolysis cell (SOEC), with high temperature steam generated from the hot syngas. The oxygen produced from the SOEC is sufficient as oxidant in gasifier, thereby eliminating the need for a cryogenic air separation unit. Compared to alkaline water electrolysis, high temperature steam electrolysis requires less electrical power. The reason for this is explained in Section 3.4.

The extra hydrogen produced is added at different process locations; most of the hydrogen is added to the syngas at high temperature and some at low temperature. At high temperature, the hydrogen is partly converting $CO_2$ to CO in a reverse water gas shift (RWGS) reaction and partly increasing the $H_2$/CO ratio. At low temperature, the hydrogen is only used to adjust the $H_2$/CO ratio to the optimal ratio. Due to reduced $CO_2$ content in the syngas, the need for $CO_2$ removal in the acid gas removal unit is substantially reduced. In order to increase the once-through conversion of syngas, and to maximize the yield of heavy wax, the Fischer-Tropsch reactor path is staged; in this case three stages as proposed by Rytter [7]. By lowering the $H_2$/CO ratio, the yield of higher hydrocarbons increases. However, the total reaction rate decreases, but the optimal ratio is lower than the stoichiometric consumption ratio. By feeding a syngas with under-stoichiometric $H_2$/CO ratio, it is necessary to feed hydrogen between the stages, and therefore we need to have some spare hydrogen to makeup for the consumption. There is a potential for optimizing the staged design with the use of a systematic method [8].

## 2. The process concepts

### 2.1. The BtL concept

Entrained flow gasification (EFG) followed by Fischer Tropsch synthesis (FTS) has been considered in the past [9–13] to be an attractive technological route for conversion of woody biomass to liquid biofuels that can meet current market specifications of fossil-based fuels. EFG technology exhibits several advantages for the integration in the production of liquid biofuels via FT synthesis. The high gas temperature in the reactor causes melting of ash and thermal cracking of tars with higher production of hydrogen and carbon monoxide [14,15]. It also enhances, in presence of steam, thermal reforming of hydrocarbons and water-gas shift of carbon monoxide, resulting in an increase of the hydrogen content in the gas product. The higher conversion of tars, as well as the hydrogen to carbon monoxide ratio that can be achieved in EF gasifiers, leads to higher carbon conversion efficiencies in the overall biomass and biofuels production process. Also, low ash and tars content in the gas product allows simpler and cheaper design of gas cleaning downstream the gasifier. On the other hand, entrained flow gasification needs a small size of the biomass particles, typically below 1 mm, for achieving high conversion rates [16]. This requires a more complex pretreatment process based on torrefaction [12] in order to improve the grindability of the biomass. The high concentration of oxygen needed for the EFG process also implies the need for an air separation unit, which increases capital cost and the electricity consumption. Despite the numerous resources and extensive research work worldwide, the progress in industrialization and commercialization of this technology has been very limited mainly due to the low carbon efficiency and the large scale requirement to make it cost-effective.

A simplified block flow diagram of a conventional BtL process is shown in Fig. 1. The biomass is pretreated to reduce particle size and moisture content. Drying of the wood chips, torrefication and grinding are the pre-treatments considered here. An alternative pre-treatment is pyrolysis where the wood is heated to a higher temperature and becomes a liquid. The torrefied wood is further converted to raw synthesis gas in an entrained flow gasifier with the addition of oxygen. Oxygen is produced by a cryogenic air separation unit, which is considered the most economical option for large scale production. The hot and reactive syngas is then quenched in a waste heat boiler (WHB) to a temperature where the gas is stable. Components like COS, $CS_2$ and HCN are hydrolyzed to form $H_2S$, $NH_3$ and $CO_2$ over a catalyst. The gas is cleaned of particles and ammonia in a water wash prior to adjusting the $H_2$/CO ratio by adding steam in a water gas shift reactor (WGS). The gas is further cooled and water is knocked out.

The acid gas removal unit is needed to remove $H_2S$, in addition to large amounts of $CO_2$. Physical absorbents, like Selexol or methanol, are

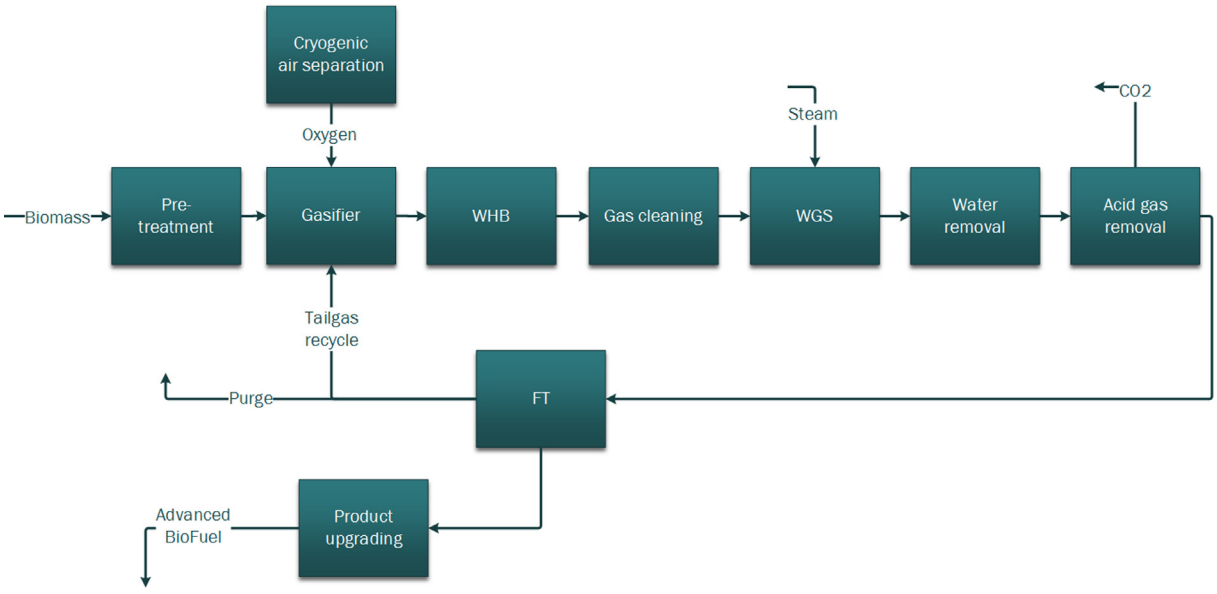


**Fig. 1.** A simplified block flow diagram of a conventional BtL process, where it is necessary to shift the syngas to increase the $H_2$/CO ratio.

suited for absorbing $CO_2$ as the partial pressure is quite high. After the dry and clean syngas is heated to a temperature of ca 210 °C, it is converted to hydrocarbons in the Fischer-Tropsch synthesis reactor. The conversion of syngas is typically 50–60%. The tailgas consists of unconverted syngas in addition to lighter hydrocarbons formed in the FT synthesis. Depending on the tailgas composition, this stream can be recycled to the gasifier and the FT reactor. In our BtL simulation, 80% of tail gas is recycled to the FT reactor because of its rich $H_2$ and CO content. A purge is required to keep the inert gas components at an acceptable level. The final step is upgrading of the Fischer-Tropsch products by hydro-treating, hydro-cracking and separation by distillation.

### 2.2. The PBtL concept

The PBtL concept proposed in this work aims to improve the carbon efficiency of the conventional BtL process presented above by introducing several modifications in the process. First, the high temperature achieved in the EF gasification process is utilized both to recycle $CO_2$ from the acid gas removal via Reversed Water Gas Shift process without the need for catalyst and to produced hydrogen via electrolysis of high temperature steam. The hydrogen production unit also produces pure oxygen, which is used for the EFG process. The Fischer Tropsch synthesis is also modified in a three-stage process introducing hydrogen between stages.

In Fig. 2, a block flow diagram of the proposed PBtL process is shown. Hydrogen and oxygen are produced by splitting steam at high temperature in solid oxide electrolysis cells (SOEC). The steam is produced in the waste heat boiler and superheated to about 700 °C. The steam is further heated to 850 °C in a fired heater, fueled by the purge gas and oxygen. The SOEC splits the water molecules and oxygen migrates through the solid oxide giving a stream of pure oxygen, while hydrogen and unconverted water are retained in the retentate stream.

In our SOEC model, 80% of water is split and the rest exits in the hydrogen rich stream. This stream is cooled down to 50 °C to condense water and a pure hydrogen stream is obtained. The hydrogen stream is reheated to about 780 °C and sent to RWGS and FT reactors. Separation of water from the hydrogen stream has advantageous effects on RWGS and FT reactions. The separated water requires no further processing and is reheated to be used in the SOEC. Pure oxygen at high temperature is highly reactive. To overcome this, it may be diluted with steam or $CO_2$ before it is fed to the gasifier.

By adding hydrogen to the syngas at high temperature in the RWGS reactor, part of the hydrogen converts $CO_2$ to CO and part of it increases the $H_2$/CO ratio. Hydrogen might also be added to the syngas at lower temperature in order to adjust the $H_2$/CO ratio to be optimal for the FT synthesis. There is no need for a WGS reactor as the $H_2$/CO ratio will be increased by adding sufficient hydrogen. The oxygen produced in the SOEC is sufficient to obtain a temperature of 1600 °C out of the gasifier, and there is no need for an expensive cryogenic air separation unit (ASU).

Another feature built into the concept is a staged FT synthesis path. The FT reactions will produce more heavy hydrocarbons at lower $H_2$/CO ratio and temperature. There is a trade-off between maximizing the selectivity to higher hydrocarbons and the production rate, and the feed composition and temperatures are optimized. Hydrogen is the limiting reactant and need to be added along the reactor path. A design with three stages is proposed where hydrogen is added prior to each stage and water and hydrocarbons are extracted after each stage. Three stage design is chosen, which gives a once-through conversion of CO higher than 90%. With such a high once-through conversion, the tailgas will consist of little syngas and there is no need to recycle to the FT reactors. The tailgas consisting of mainly lighter hydrocarbons is recycled to the gasifier. Since there is little $CO_2$ in the syngas after the RWGS, the main purpose of the acid gas removal unit is to remove $H_2S$. However, some $CO_2$ is extracted along with the sulphur. The effect of $CO_2$ extraction on FT production is explained in Section 4.

A more detailed process flow diagram of parts of the PBtL process is shown in Fig. 3. The waste heat boiler quenches the hot and reactive syngas to a temperature where it is chemically stable. The heat released produces high pressure steam by evaporating water at ca 117 bar and 322 °C, which is further superheated to 730 °C. Part of the high pressure steam is used in the pretreatment of the biomass, while the main part is applied as feed to the SOEC. The SOEC will not withstand a pressure of 117 bar, so the pressure is reduced over a reduction valve to 40 bar, which is the chosen design pressure. The steam is further heated in a

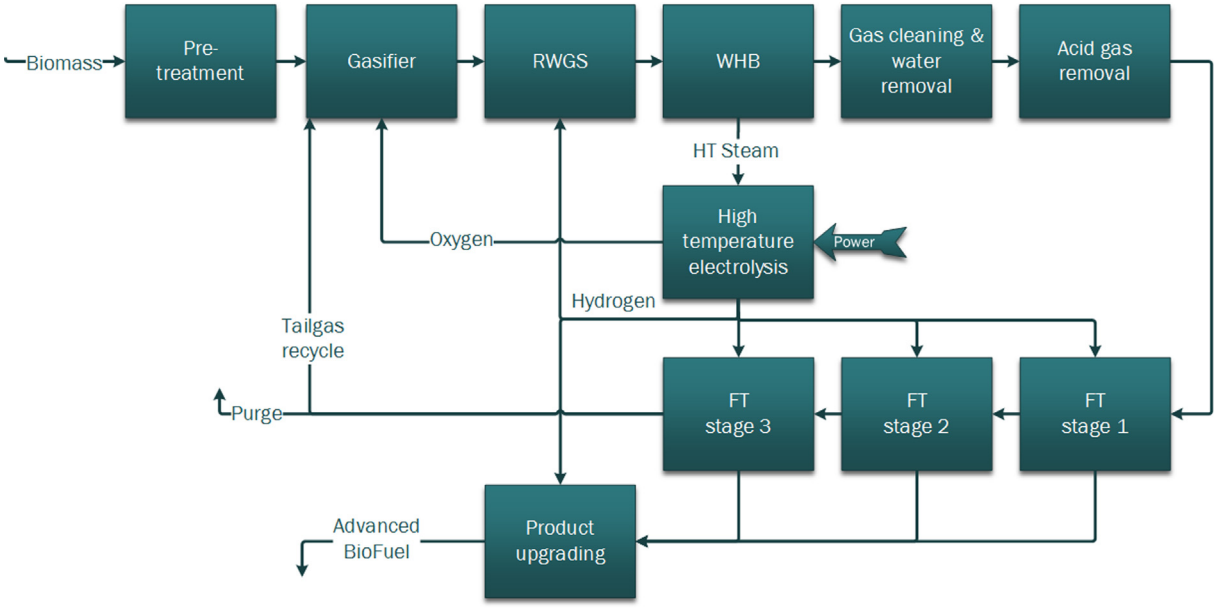


**Fig. 2.** A simplified block flow diagram of the proposed PBtL process, where hydrogen produced from high temperature steam electrolysis is added at both high an low temperature.

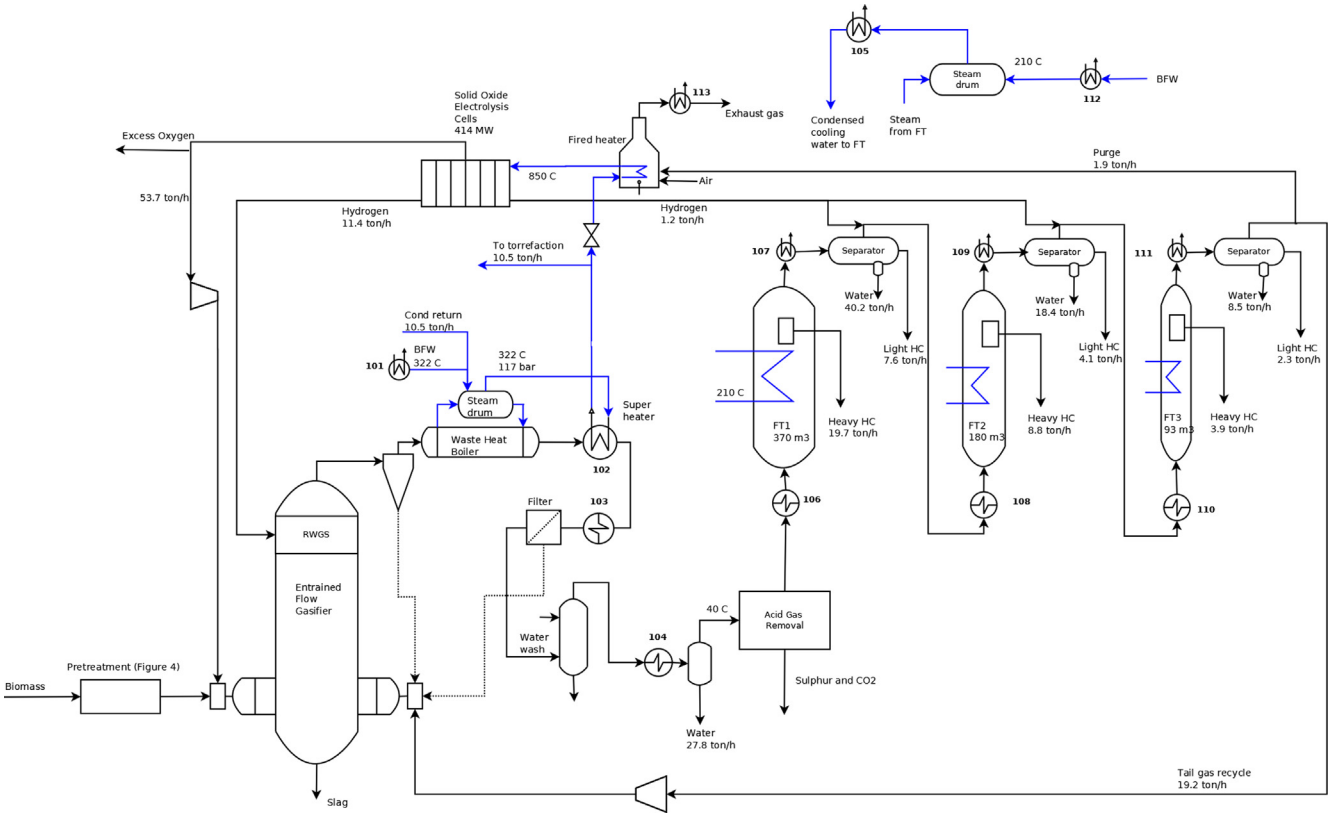


**Fig. 3.** Process flow diagram of the proposed PBtL process. The steam system is shown in blue. The product upgrading is not shown. The heat exchangers shown with a tag number are included in composite curve (Fig. 17). (For interpretation of the references to colour in this figure caption, the reader is referred to the web version of this article.)

fired heater to 850 °C before it enters the SOEC.

### 2.3. Biomass pretreatment

Fig. 4 shows a schematic representation of the main process steps considered in the biomass pretreatment system, which includes drying, torrefaction and grinding. The proposed design is integrated with the overall process of the plant, where the flue gas from the fire heater and the tail gas from FTS are used as heating medium for the dryer and the torrefaction respectively. Superheated steam produced from the heat recovery in the syngas cooling system is used to preheat the tail gas before torrefaction. The volatiles released from the torrefaction process are taken, together with the tail gas, to the EF gasifier. The torrefaction process has already been shown in the past to be necessary when considering EF gasification of wood [12,16] in order to improve the grindability of the wood [17,18] and achieve a particle size distribution

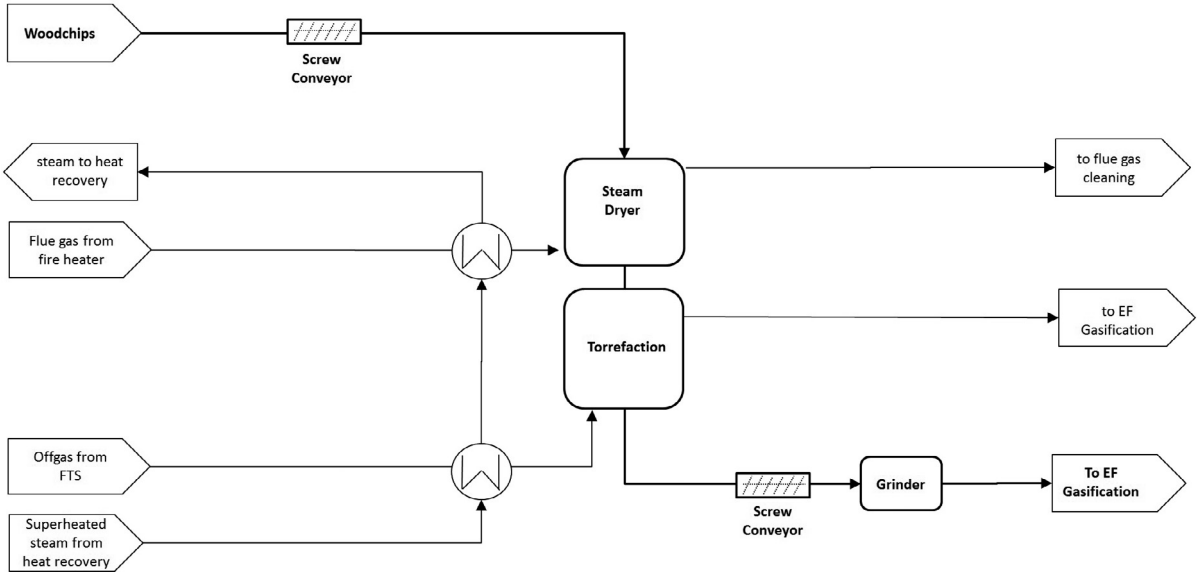


**Fig. 4.** Schematic representation of the biomass pretreatment process design considered in this work, which includes drying, torrefaction and grinding as main process steps.

[19] suitable for EF gasification (typically below 0.5 mm).

### 2.4. Entrained flow gasification

Thermochemical conversion of the biomass is performed in high temperature oxygen-enriched entrained flow (EF) gasification. Considering integration in the production of liquid biofuels via FT synthesis, entrained flow gasification technology exhibits a number of advantages relative to fixed-bed or fluidized-bed gasification [16]. The high gas temperature in the reactor causes melting of ash and thermal cracking of tars with higher production of hydrogen and carbon monoxide [14,15]. It also enhances, in presence of steam, thermal reforming of hydrocarbons and water-gas shift of carbon monoxide, resulting in an increase of the hydrogen content in the gas product. The higher conversion of tars, as well as the hydrogen to carbon monoxide ratio that can be achieved in EF gasifiers, leads to higher carbon conversion efficiencies in the overall biomass and biofuels production process. Also, low ash and tars content in the gas product allows simpler and cheaper design of gas cleaning downstream the gasifier. On the other hand, entrained flow gasification requires smaller particle size, typically below 1 mm, in order to achieve high conversion rates [16].

The overall EF gasification process is described in terms of the gasification reactor pressure and temperature, the lambda value or air-fuel equivalence ratio, and the steam to carbon ratio. The lambda value is defined as the ratio between the actual molar flow rate of oxygen used for gasification to the total stoichiometric flow rate needed for complete biomass combustion. Lower and upper operational limits for the gas temperature in the entrained flow gasification are specified with constant values equal to 1300 and 1600 °C, respectively. The lower temperature limit is considered in order to ensure complete ash melting [20], while the upper temperature limit corresponds to technical constrains in refractory materials that are commercially available at reasonable prices. The lambda value considered for the gasification is within the range of 0.2–0.4. This has been established as an optimal range for oxygen-enriched gasification [14,21,22] to achieve complete char gasification as well as partial oxidation of the high-chain hydrocarbons and poly-aromatics produced during decomposition of the volatiles fraction of the biomass.

### 2.5. Acid gas removal

For the PBtL concept, removal of $H_2S$ is required in order to reach the feed gas specification needed for FT synthesis, here specified to be 10 ppb [2]. Also, $H_2$ and CO losses during the acid gas removal should be minimized in order to retain the desired $H_2$/CO ratio for FT synthesis. Considering these requirements, acid gas removal based on physical solvents [23–26] has been selected. Among the commercially available physical solvents, Selexol has been chosen since it allows pure pressure-swing process configurations without the need for intensive solvent refrigeration or thermal regeneration. This enables substantial savings in energy consumption. The process flow diagram of the $H_2S$ removal process is shown in Fig. 5. The syngas is initially water-cooled to 25 °C and free water is removed in a water knock-out drum. The syngas then enters the absorber where the Selexol solvent, pre-cooled to 25 °C by cooling water, is sprayed in counter-current. The rich solvent is then regenerated in by flashing and stripping. The gas from the flash drum contains considerable amounts of hydrogen and CO, and is therefore recycled back to the absorber to minimize the losses of these components. After the stripper, the rich selexol is pumped and cooled back to the absorber. The concentration of $H_2S$ achieved by the selexol system is 1 ppm. Further reduction of the $H_2S$ to the FTS requirements is performed in by adsorption in a ZnO bed.

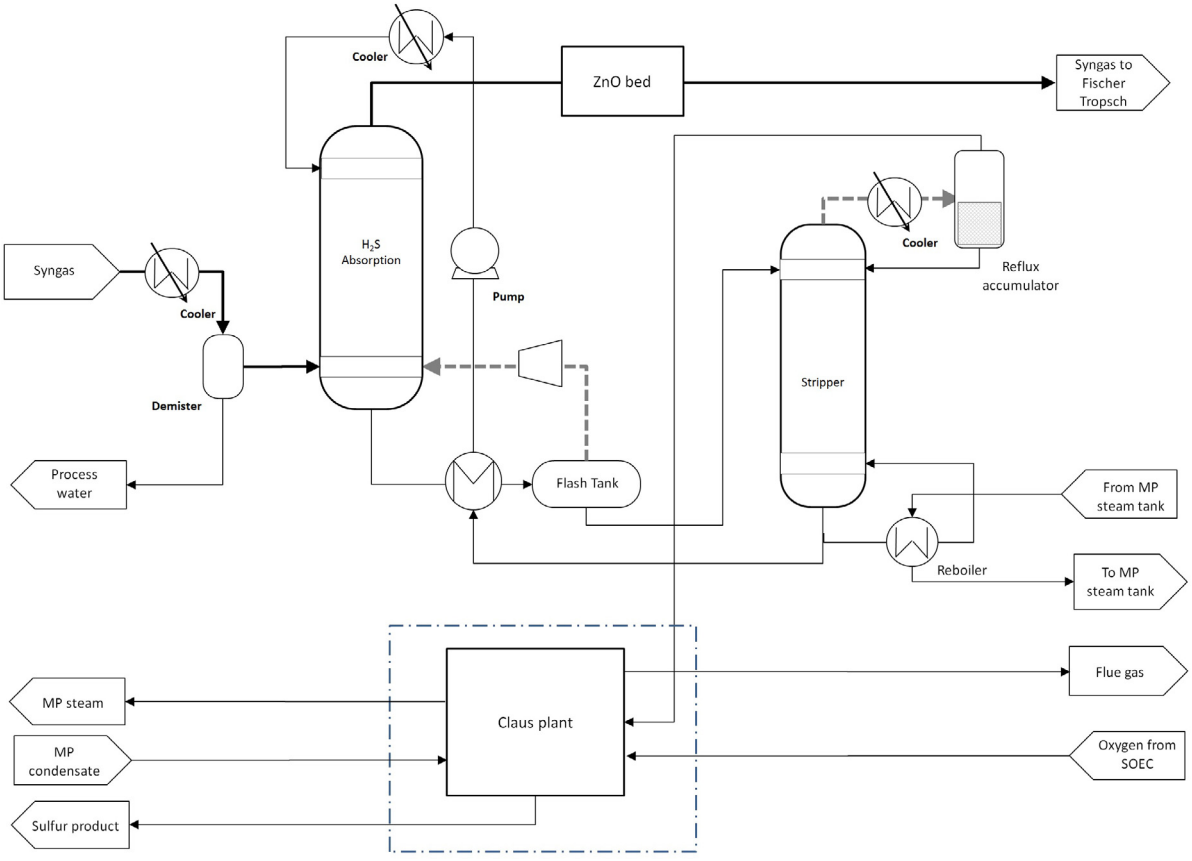


**Fig. 5.** A simplified block flow diagram of the acid gas removal system, based on one single absorber for $H_2S$ from the raw syngas.

### 2.6. Hydrogen production

There are several alternative technologies for producing hydrogen from electrical power; where alkaline water electrolysis (AWE), proton exchange membrane water electrolysis (PEMWE), solid oxide electrolysis cell (SOEC), and molten carbonate electrolysis cell (MCEC) can be considered as the most important ones [27]. Among these technologies SOEC is the one that has the best energy efficiency in combination with being relative matured. SOEC is today a commercially available system. The reason for the high energy efficiency is that at elevated temperatures, the kinetics of the cell is very high. In combination with use of residual heat, the electric efficiency can even exceed 100%, as the minimum needed electric work decreases as temperature increases. Because SOEC using yttria doped zirconia oxide is technologically matured and because of the low electric energy demand in combination with waste heat, we have chosen to use SOEC in the PBtL system described here.

### 2.7. Fischer-Tropsch synthesis

Fischer-Tropsch Synthesis (FTS) is a polymerization reaction from synthesis gas (syngas), a mixture of hydrogen and carbon monoxide. The products with a cobalt based catalyst are mainly straight chain paraffins and $\alpha$-olefins. FTS has been developed industrially since 1925 and can be considered a mature technology, though there are still developments going on [28]. During the last three decades several natural gas-to-liquid plants have been built in Qatar, Malaysia and Nigeria with Shell and Sasol technologies. Employed reactor technologies for these two companies are tubular fixed-bed and slurry bubble-column, respectively. Other reactor technologies have been tested extensively on a smaller scale, notably the fixed-bed microchannel reactor. These reactors have several pros and cons, encompassing the well-proven tubular fixed-bed, and the highly scalable slurry reactor with excellent heat removal capacity. For the present study, we have selected the slurry bubble-column reactor. It is characterized by close to full back-mixing of the gases and liquid products, meaning that the catalyst is exposed to the exit gas composition throughout the entire reactor. This has the advantage of improved selectivity to higher hydrocarbons due to a low $H_2$/CO ratio and high water vapor pressure [29], but comes at the expense of lower partial pressure of the reactants. All modern FT plants uses a catalyst based on cobalt due to high selectivity, high activity, robustness and very low water-gas-shift (WGS) activity. This means that the overall $H_2$/CO consumption ratio is ca. 2.15, slightly depending on variations in polymerization probability from one catalyst to another, the actual process conditions, and selectivity distribution between olefins and paraffins. Minor amounts of oxygenated byproducts are neglected in the present simulations. However, the inlet $H_2$/CO ratio to the FT reactor(s) preferentially is lower than the overall consumption ratio, meaning that this ratio becomes even lower as the reaction proceeds. The rationale for this choice of conditions is that the selectivity to higher hydrocarbons strongly depends on the $H_2$/CO ratio and it is desirable to suppress formation of methane and light hydrocarbons. The CO conversion in an FT slurry reactor is limited to the range 60–65% [2,29,30]. Important limiting parameters in the design are heat-removal, linear gas velocity, catalyst activity and reactor length. Further, at very high conversions the partial pressure of water becomes sufficiently high to impose danger of accelerated deactivation through cobalt oxidation and enhanced WGS activity, in addition to exceedingly low syngas partial pressure. For this reason, we have staged FT reactor-block with three consecutive stages (Fig. 2). Water is knocked-out and liquid FT products are separated after each reactor and the syngas composition adjusted to become approximately equal at each reactor inlet by adding some hydrogen. With 55% conversion in each reactor, the total once-through CO conversion becomes nominally 91.0%. A high once-trough conversion reduces the need for recycle of unconverted syngas and simplifies handling of byproducts and inerts. Liquid hydrocarbons are continuously extracted through filters incorporated in the slurry reactors. A small portion of the tail gas is purged to remove unconvertable nitrogen from the system. The purge is used as fuel to further heat the high pressure steam. This is also where most of the carbon is lost from the system. The bulk of the tail-gas is recycled to the gasifier to convert $CO_2$, methane and light hydrocarbons to syngas. Note that the present concept avoids recycle directly to the FT-reactor block, and thus allows a certain enhanced amount of inert $CO_2$ to be present in the syngas.

### 2.8. The reverse water gas shift reactor

The reverse water gas shift reaction is endothermic. High temperature is beneficial, as the reaction will equilibrate faster and the equilibrium is driven towards CO production.

$$H_2 + CO_2 \rightleftharpoons CO + H_2O \quad (1)$$

In the present concept, the RWGS reaction is performed as an upper section of the entrained-flow gasifier by adding hydrogen to the already equilibrated gas. Due to the endothermic nature of the RWGS reaction and addition of a colder gas, the temperature drops from ca. 1400 °C and below the critical softening temperature of steel of 1100 °C, [29] e.g. to 1000 °C. By using such chemical quenching, traditional water quenching is avoided. Further cooling of the shifted gas is performed by a conventional waste-heat boiler and a superheater, generating high temperature steam for the electrolysis and the pretreatment units. By adding hydrogen to the syngas, some methane is also formed. The methanation reaction is exothermic, and less methane is formed at higher temperatures. For these reasons, the temperature in the RWGS reactor should be as high as feasible. At temperatures above 900 °C, a catalyst is, from kinetic calculations, not expected to be necessary.

Due to the significant amount of steam that is present at the top of the gasifier, it is assumed that the risk of coking by the Boudouard reaction is minimal.

$$2CO \longrightarrow CO_2 + C \quad (2)$$

However, this needs to be proven. Although the RWGS reaction seems to be a rather conventional gas phase reaction, there is limited literature on the subject and no known commercial experience. For that reason, RWGS is considered to be unproven technology at moderate TRL (Technology Readiness Level).

### 2.9. Upgrading of FTS products

The products from the FTS are fractionated based on the carbon number to light gases ($C_1$-$C_4$), naphtha ($C_5$-$C_{10}$), middle distillate ($C_{11}$-$C_{19}$) and wax ($C_{20+}$). In order to evaluate the economics, it has been assumed that the plant design includes a refining of the middle distillate and wax from the FTS by hydrotreating and hydrocracking, respectively [31–33]. The hydrotreating unit is producing diesel and light gases with 98.5 and 0.9% wt. yields [34], respectively. The hydrocracking unit produces diesel, kerosene, naphtha and light gases with 75.5, 17.2, 4.0 and 5.0% wt. yields [34,35]. The products from the refining are separated in one atmospheric distillation column to commercial-grade kerosene (jet fuel), diesel and naphtha. The naphtha from the distillation column is mixed with the naphtha separated from the FTS products and sold. Light gases are cooled with separation of the LPG ($C_2$-$C_4$), sold as by-product, and the remaining gas is mixed with the tail gas from FTS.

## 3. Process modeling and simulation

Aspen HYSYS® V9 is used as a modeling and simulation tool of the process flowsheets in this study. The Fisher-Tropsch reactors are not modeled by existing modules inside Aspen HYSYS, due to the need for more detailed models of the reaction stoichiometry and kinetics. MATLAB CAPE-OPEN unit operation [36] is used for this purpose.

### 3.1. Biomass characterization, pretreatment and gasification

The biomass as a chemical component, is introduced as a solid hypothetical component in Aspen HYSYS with the elemental composition given in Table 1. By estimation the weight based heat of formation [kJ/kg] from the elemental composition based on the method of Burnham [37], the required molar heat of formation is specified to be $-5.184{\cdot}10^5$ kJ/kmol, with an arbitrary molar mass of 100.11 kg/kmol. The wet biomass is assumed to have 40% moisture content, which reduces to 5% after pretreatment; drying and torrefaction.

The drying process is evaluated in terms of the total flow rate of water evaporated and the required input thermal power of the drying agent, which is assumed to be 2.8 GJ/ton $H_2O$, with the temperature of the drying agent equal to 150 °C. The MP steam available from the FT synthesis is more than enough to cover this energy sink. Fig. 17 shows that we have more than 150 MW heat available at ca 200 °C and the required heat for the drying is ca 25 MW. The torrefaction process is evaluated based on the yields obtained experimentally by Tapasvi et al. [38], assuming the temperature and the residence time in the torrefaction reaction equal to, respectively, 275 °C and 30 min. The design of the torrefaction reactor is based on a vertical cylindrical tower with a height to diameter ratio equal to 2 and a solid to gas volume ratio equal to 0.82. The electricity consumption by the grinder is based on the linear correlation as a function of the torrefaction temperature obtained experimentally by Govin et al. [39], which corresponds to 50 kWh/ton for the assumed torrefaction temperature.

The gasifier is modeled by two reactors; one conversion reactor where the biomass is decomposed into C, $H_2$, $N_2$, $O_2$ and S, with a stoichiometry given by the biomass elemental composition. A second reactor takes the products from the decomposition along with added oxygen and water and calculates the equilibrium composition by minimizing the Gibbs free energy. The heat released from the equilibrium reaction must at least be the heat required of the decomposition reaction, and the amount of oxygen is adjusted so that the temperature is at the desired temperature level. Since the gasifier is large, the relative heat losses are small and is neglected here. This gives the chemical equilibrium of an adiabatic gasifier.

As long as the temperature is relatively high, which is the case for an entrained flow gasifier, the assumption of chemical equilibrium of the gas and negligible tar are reasonable assumptions. The gasifier is operating at 1600 °C and 40 bar.

### 3.2. The reverse water gas shift reactor

In the flowsheet simulation, the RWGS reactor is modeled as an equilibrium reactor by minimization of Gibbs free energy. Hence, the assumption is that the volume is large enough to reach equilibrium.

With a pure and homogeneous gas phase reaction, it is possible to calculate how fast the gas will reach equilibrium after hydrogen is added. Based on the kinetic model Gri-Mech 3.0 [40], dynamic simulation of the homogeneous gas phase reactions is made.[2] The model is implemented in Cantera [41,42] with the use of Python programming language. The model is a compilation of 325 elementary chemical reactions, and associated rate coefficient expressions and thermochemical parameters for the 53 species involved in them.

The Figs. 6 and 7 show how fast the homogeneous gas phase reactions approach equilibrium when syngas from the gasifier is mixed with hydrogen, starting at 1100 °C and 1200 °C, respectively. The residence time can be reduced from 3 s to 0.5 s, and hence the volume of the RWGS may be reduced by a factor of 6 by increasing the temperature from 1100 °C to 1200 °C. For the capacity used here, the volume of the RWGS is about 12 $m^3$ for a 0.5 s residence time. To reduce the volume even more, the reaction may be catalyzed by introducing a solid surface.

[2] GRI-Mech 3.0 is an optimized mechanism designed to model natural gas combustion, including NO formation and reburn chemistry.

### 3.3. Fischer-Tropsch reactor

In this study, the slurry bubble-column FT reactor is modeled as a completely stirred tank reactor (CSTR). The syngas has a pressure of about 37 bar prior to the first FT reactor and a temperature of 210 °C at the feed to all FT reactors. The polymerization reactions taking place are hydrogenation of CO to form n-paraffins, 1-olefins and oxygenates.

$$n\mathrm{CO} + (2n+1)\mathrm{H_2} \rightarrow \mathrm{C}_n\mathrm{H}_{2n+2} + n\mathrm{H_2O} \quad n = 1, 2, \ldots, \infty \tag{3}$$

$$n\mathrm{CO} + 2n\mathrm{H_2} \rightarrow \mathrm{C}_n\mathrm{H}_{2n} + n\mathrm{H_2O} \quad n = 2, 3, \ldots, \infty \tag{4}$$

$$n\mathrm{CO} + 2n\mathrm{H_2} \rightarrow \mathrm{C}_n\mathrm{H}_{2n+2}\,\mathrm{O} + (n-1)\mathrm{H_2O} \quad n = 1, 2, \ldots, \infty \tag{5}$$

More than 90% of the products are paraffins and the rest is mainly olefins. The oxygenates are neglected here as they are formed only in small amounts. These reactions do not account for the product distribution unless we describe the individual reaction rates. A common assumption and observation is that the ratio of two consecutive reaction rates is given by a parameter, the chain growth factor or the propagation probability, $\alpha$. The chain growth factor for paraffins is larger than that for the olefins, as the long chain hydrocarbons are mainly paraffinic while among the short more olefins are observed. The formation reactions of paraffins and olefins are lumped into two separate reactions, where the stoichiometric coefficients are given by the Andersen-Schulz-Flory (ASF) distribution and with two different growth factors, $\alpha_1$ and $\alpha_2$. In addition, the selectivity to methane is higher than predicted by the ASF distribution and the selectivity towards ethylene is lower. Therefore two extra reactions are introduced to account for the observed distribution. The following reactions and lumps are included in the kinetic model:

$$\mathrm{CO} + U_1\,\mathrm{H_2} \xrightarrow{r_1} \nu_{1,1}\mathrm{CH_4} + \nu_{1,2}\mathrm{C_2H_6} + \cdots + \nu_{1,10}\mathrm{C_{10}H_{22}} + \nu_{1,[11,\infty]}\mathrm{C}^{\mathrm{p}}_{11+} + \mathrm{H_2O} \tag{6}$$

$$\mathrm{CO} + U_2\,\mathrm{H_2} \xrightarrow{r_2} \nu_{2,1}\mathrm{CH_4} + \nu_{2,2}\mathrm{C_2H_4} + \cdots + \nu_{2,5}\mathrm{C_5H_{10}} + \nu_{2,[6,\infty]}\mathrm{C}^{\mathrm{o}}_{6+} + \mathrm{H_2O} \tag{7}$$

$$\mathrm{CO} + 3\mathrm{H_2} \xrightarrow{r_3} \mathrm{CH_4} + \mathrm{H_2O} \tag{8}$$

$$\mathrm{C_2H_4} + 2\mathrm{H_2} \xrightarrow{r_4} 2\mathrm{CH_4} \tag{9}$$

The growth factor $\alpha_2$ is ca 70% of $\alpha_1$, and therefore the olefin lump is lighter than the paraffin lump [43]. For a given catalyst, the growth factors will change with the $H_2$/CO ratio, the temperature and the water partial pressure. A consistent procedure [44] for calculating the stoichiometry is applied, giving the following stoichiometric coefficients:

$$\nu_{1,i} = (1-\alpha_1)^2\alpha_1^{i-1} \tag{10}$$

$$\nu_{1,[11,\infty]} = (1-\alpha_1)\alpha_1^{10} \tag{11}$$

$$\nu_{2,i} = (1-\alpha_2)^2\alpha_2^{i-1} \tag{12}$$

$$\nu_{2,[6,\infty]} = (1-\alpha_2)\alpha_2^{5} \tag{13}$$

**Table 1**
The elemental composition of the biomass feedstock.

| Element | Wt% dry basis |
|---|---|
| C | 51.8 |
| H | 6.04 |
| N | 0.17 |
| S | 0.09 |
| O | 41.9 |

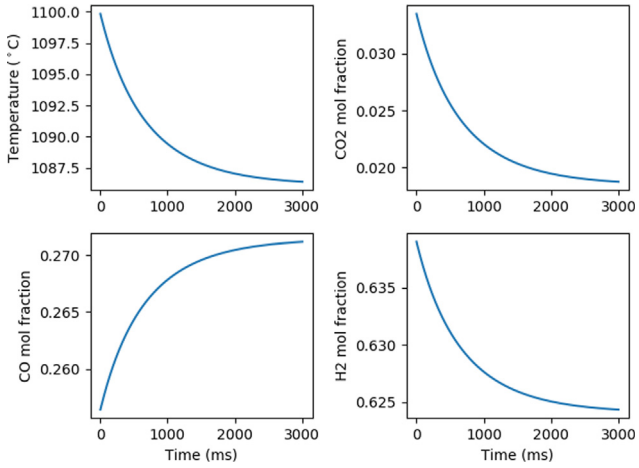


**Fig. 6.** The dynamics of the homogeneous RWGS reactor starting at 1100 °C.

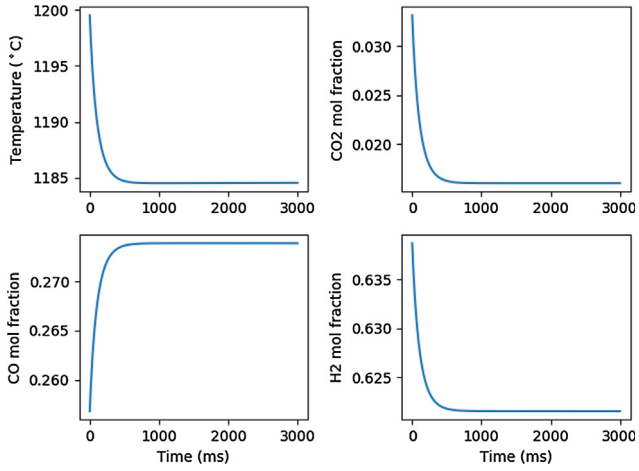


**Fig. 7.** The dynamics of the homogeneous RWGS reactor starting at 1200 °C.

$$U_1 = 3-\alpha_1 \tag{14}$$

$$U_2 = 2 + (1-\alpha_2)^2 \tag{15}$$

The molecular weights of the lumps are not constant, but will vary with $\alpha_1$ and $\alpha_2$. In a simulation system like Aspen HYSYS or any other system, a hypothetical component must have a constant molecular weight. Since the molecular mass of the lumps above will vary, each lump is modeled by three hypothetical components with a given constant molecular mass. The distribution between the lumps follows the ASF distribution and such that the mass is conserved. Since the growth factors are not constant, but rather functions of the $H_2$/CO ratio, the partial pressure of $H_2O$ and the temperature, the existing unit models in Aspen HYSYS cannot be used. The FT reactor model is written in MATLAB and implemented in Aspen HYSYS through MATLAB CAPE-OPEN unit operation. A reaction rate model published by Outi et al. [45] and a chain growth model published by Ostadi et al.[46] are refitted to the CSTR experimental data of Todic et al. [43] and used in the simulations.

### 3.4. Modeling the solid oxide electrolysis cell

Solid oxide electrolysis cell, SOEC, is based on splitting water in a vapour state into oxygen and hydrogen. Doing so, hydrogen is reduced electrochemically via Eq. (16). The oxygen ions produced at the cathode migrate via a solid electrolyte to the anode, where the oxidation reaction in Eq. (17) takes place. The solid oxide electrolyte acts like a membrane in that it is only permeable to one component or specie ($O^{2-}$) and rejects everything else ($H_2$, $H_2O$, and $O_2$). The cathode and anode reactions are given by Eqs. (16)and (17), correspondingly.

$$H_2O_{(g)} + 2e^- \longrightarrow H_{2(g)} + O^{2-} \tag{16}$$

$$O^{2-} \longrightarrow \frac{1}{2}O_{2(g)} + 2e^- \tag{17}$$

The first law of thermodynamics, $W_{el}-Q + H_{in} = H_{out}$, applied to the SOEC process becomes:

$$\dot{n}X2FE^{rev} + \dot{n}X2FIR_{elt} + \dot{n}h^{in}_{H_2O} = \dot{n}Xh^{out}_{H_2} + \dot{n}\frac{X}{2}h^{out}_{O_2} + \dot{n}(1-X)h^{out}_{H_2O} \tag{18}$$

Since $\dot{n}X2F = I$, where $I$ is the current applied to the SOEC, $\dot{n}$ the molar feed rate of steam to the cell, $F$ is the Faraday constant, 2 is the number of electrons exchanged per water molecules and $X$ is the conversion degree of steam, the model is reduced to:

$$IE^{rev} + I^2R_{elt} + \dot{n}\Delta_{in-out}h_{H_2O} = \dot{n}X\Delta h_{react} \tag{19}$$

$$\dot{n}X\Delta h_{react} = \dot{n}X\Delta g_{react} + \dot{n}XT^{out}\Delta s_{react} \tag{20}$$

$$0 = (\dot{n}X\Delta g_{react}-IE^{rev}) + (\dot{n}XT^{out}\Delta s_{react}-I^2R_{elt}-\dot{n}\Delta_{in-out}h_{H_2O}) \tag{21}$$

Here, $\Delta_{in-out}h_{H_2O}$ is the sensible heat brought in and out of the process by the feed steam, $T^{out}\Delta s_{react}$ is latent heat adsorbed and carried out by the reaction products, $\dot{n}X\Delta g_{react}$ is the electric work accumulated by the products and is identical to $IE^{rev}$ being the added reversible electric work. The term $I^2R_{elt}$ is the irreversible Ohmic heat generated in the cell and $R_{elt}$ is the Ohmic resistance mainly from the electrolyte of the SOEC.

The Ohmic resistance in the SOEC can to a reasonable approximation be regarded as the only significant irreversible term in this process and it is given by Eq. (22);

$$R_{elt} = \frac{\delta_{elt}}{\sigma_{elt}}\frac{1}{A_{elt}} \tag{22}$$

where $\delta_{elt}$ is electrolyte thickness, $\sigma_{elt}$ is electrical conductivity, and $A_{elt}$ is electrolyte in-plane area. The term $I^2R$ term is a key energy term in an SOEC cell for at least two reasons; it dictates the electric energy input and also the need for other heat sources. This Ohmic heat term depends on the geometry of the cell ($\delta_{elt}$ and $A_{elt}$), but also heavily on the operation temperature as the conductivity follows an Arrhenius temperature behaviour. The ionic electric conductivity, $\sigma_{elt}$, of $Y_{0.2}Zr_{0.8}O_2$ is tabulated in Table 2.

**Table 2**
Conductivity of the selected SOEC membrane as a function of temperature and ohmic potential drop, $IR$, at 1 kA m$^{-2}$ and for 50 μm thick membrane [47]. The table also lists the reversible heat potential and the electric potential [48].

| $T$/°C | 25 | 560 | 597 | 636 | 727 | 838 | 903 | 977 | 1060 | 1156 |
|---|---|---|---|---|---|---|---|---|---|---|
| $\sigma_{elt}$/S m$^{-1}$ | – | 0.2 | 0.4 | 0.8 | 2 | 6 | 9 | 10.5 | 13 | 15 |
| $IR$/V | – | 0.250 | 0.125 | 0.063 | 0.025 | 0.008 | 0.006 | 0.005 | 0.004 | 0.003 |
| $-\frac{T\Delta s}{2F}$/V | – | 0.24 | 0.25 | 0.26 | 0.30 | 0.33 | 0.36 | 0.38 | 0.41 | 0.43 |
| $E^o = -\frac{\Delta g^o}{2F}$/V | 1.23* | 1.05 | 1.04 | 1.02 | 1.00 | 0.96 | 0.94 | 0.92 | 0.90 | 0.88 |

* Refers to hydrogen and oxygen gases and liquid water.

The heat balance of an SOEC is crucial for operation temperature and is dictated by three factors; the heat needed reversibly in the reaction, $\dot{n}XT\Delta s$, the heat generated irreversibly by Ohmic resistance (ionic friction) in the membrane (solid oxide electrolyte), $I^2R$, and finally the sensible heat from the feed steam. The heat balance can be summarized by Eq. (23);

$$-\dot{n}XT^{out}\Delta s_{react} = I^2R_{elt} + \dot{n}\Delta_{in-out}h_{H_2O} \quad (23)$$

Considering only the entropic reversible heat term and Ohmic heat term, the cell will balance itself on a temperature where the two terms are of the same size. This temperature is the thermoneutral temperature, $T_{TN}$. That is, at any given constant current, $I$, if the cell is too cold, the resistance will be so high (due to low conductivity at low temperature) that the cell will self heat to the temperature where the Ohmic resistance is lower and the Ohmic heat is adsorbed by the entropic heat need, $T\Delta s$. If, on the other hand, the operational temperature is above the thermoneutral temperature, the Ohmic resistance will drop (due to higher conductivity at higher temperature) and the entropic heat requirement is not fulfilled and the SOEC becomes self cooling until the thermoneutral temperature, $T_{TN}$, is met. Under thermoneutral temperature conditions the cell operates adiabatically, as it does not exchange heat with the environment. This, adiabatic conditions, is the assumption for which we model and consider the SOEC in our PBtL model.

Operating an SOEC away from the thermoneutral temperature requires additional heating or cooling. This can be provided by adding steam at a temperature different than the thermoneutral temperature. In the case of PBtL excess heat from the gasifier is available and can be used to heat steam to temperatures well above 1000 °C. When feeding this hot steam to an SOEC, the operation temperature becomes so high that the Ohmic resistance is almost absent and the electric work needed becomes close to Gibbs free energy. Gibbs free energy of hydrogen formation from water is closer to zero (less negative) at higher temperature and this allows for electric input that is lower than what is needed at room temperature. This is shown in Table 2. Thus the electric efficiency becomes more than 100%, or super high (super refers to higher than 100%). The energy efficiency is still defined by the relation between the reaction enthalpy and Gibbs free energy. The point here is that combining waste heat with solid oxide electrolysis and feeding this hydrogen into an RWGS and Fischer Tropsch Synthesis (FTS) allows for extremely efficient, carbon neutral and renewable energy based production of synthetic fuels like, gasoline, diesel and Jet-A.

$$\Delta_{in-out}h_{H_2O} = X(-T^{out}\Delta s_{react} - 2FIR) \quad (24)$$

Utilizing waste heat for reduced specific power need can be obtained when the inlet vapour is at much higher temperature than the thermoneutral or outlet temperature ($T^{out}$ or $T^{TN}$). In this case, the vapour will be cooled to the operation temperature, $T^{out}$, while passing through the SOEC. This cooling changes the enthalpy of the vapour in the process, $\Delta_{in-out}h_{H_2O}$, and will compensate for the heat deficit between the reversible, $T\Delta s$, and the irreversible heat, $zFIR$. That is, sensible heat from the change in enthalpy in the inlet steam together with heat from the ohmic resistance compensates for the reversible heat need in the reaction. Looking at Eq. (24), the enthalpy difference in and out, $\Delta_{in-out}h_{H_2O}$, can be calculated for a given conversion rate, $X$ and a given SOEC in operation. Taking this enthalpy change value, one can find the inlet temperature as function of the outlet temperature. In Fig. 8 (right), this is done for conversions of 0.2, 0.5, and 0.8 for an SOEC with 50 µm thick membrane electrolyte and a current density of 1 kA $m^{-2}$.

As an example, see the left graph in Fig. 8, consider inlet steam of 850 °C and 20% conversion. From the right axis this temperature is plotted horizontally (dashed, dark yellow) towards the 0.2 conversion line (dark blue) and vertically down from the intersection point. In this way one can read that a steam inlet temperature of 850 °C and 20% conversion gives an outlet temperature of 650 °C. By taking a horizontal line (dotted, dark yellow) from where the out temperature vertical line (dashed, dark yellow) intercepts with the cell potential (dash-dot, green) towards the left axis, one can read the electric energy need, which for this example is 28.8 kWh $kg_{H_2}^{-1}$.

This use is based on considering that the electrolyte holds uniform temperature inside the SOEC. This simplification considers that it is the outbound temperature that dictates the entire solid oxide electrolyte. However and in practise, parts of the electrolyte will be at a higher temperature, in turn leading to a higher need for heat at the inlet region. In turn there will be less heat available at the outlet region, where more electricity is applied. This is close linearly coupled and means that the system models adds up as more heat and less electricity is spent at the inlet of the SOEC and *vice versa* at the outlet. In this respect, the model here gives a fair assessment of the need for electricity and heat of an SOEC operating away from a thermoneutral condition.

## 4. Simulation results

### 4.1. The effect of adding hydrogen

As mentioned in the introduction, hydrogen is added at different locations of the PBtL process; prior to the RWGS reactor and prior to each FT reactor. With 90% of the unconverted $CO_2$ extracted in the acid gas removal unit, Fig. 9 shows the effect of distributing the hydrogen between the RWGS and FT reactors on the total production. With no addition of hydrogen to the RWGS, there is a need for ca 5300 kmol/h of hydrogen to FT reactors in order to make up for the low $H_2$/CO ratio from the gasifer. By adding that much hydrogen, the $H_2$/CO ratio is increased to the desired level, and the water gas shift is avoided and hence a substantial loss of CO. As the hydrogen addition is shifted to the

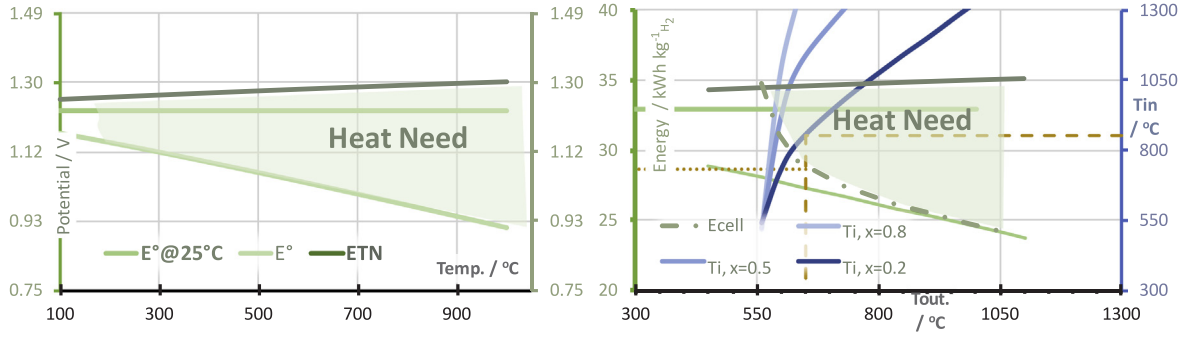


**Fig. 8.** Energy and temperature overview. LEFT: Standard potential (V) as function of temperature, standard potential (V) at room temperature, and thermoneutral potential (V) as function of temperature. RIGHT: Specific work, heat, and total energy. Blue lines indicate inlet vapour temperature to meet heat demand at different operation temperatures. 1.49 V is the same amount of energy as 40 kWh $kg_{H_2}^{-1}$. (For interpretation of the references to colour in this figure caption, the reader is referred to the web version of this article.)

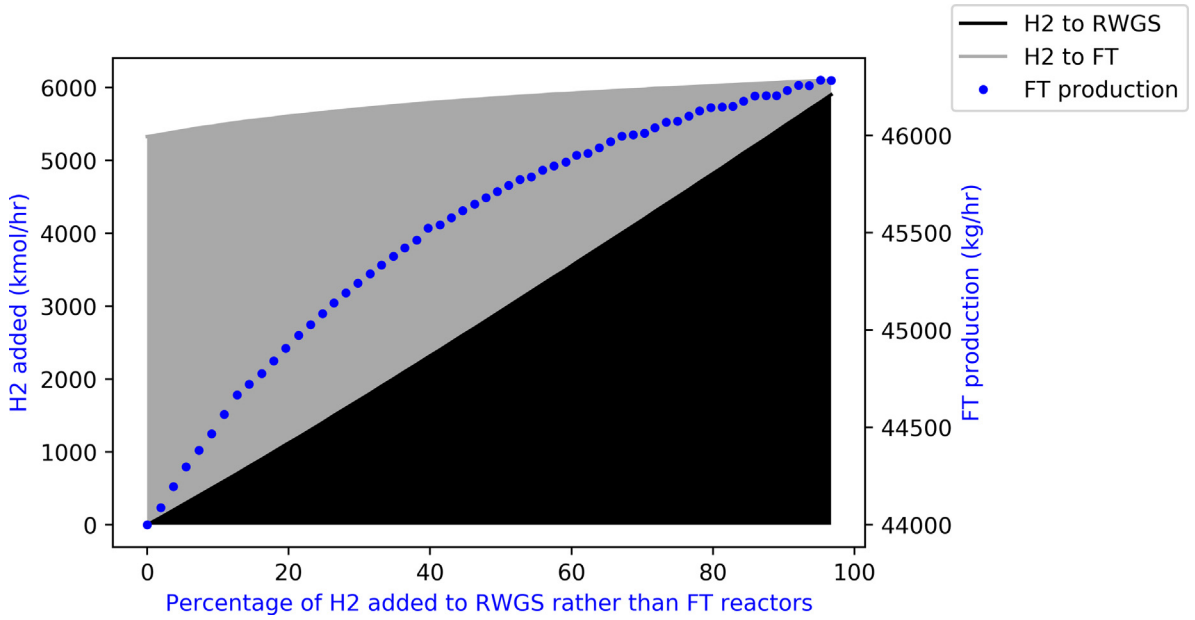


**Fig. 9.** Effect of distributing the hydrogen between RWGS and FT reactors in PBtL process. In all cases the $H_2$/CO ratios to the FT reactors are the same. 90% of $CO_2$ is extracted in acid gas removal unit.In case with no $H_2$ added to RWGS (0%), there is still a need for hydrogen addition to FT reactors to increase the $H_2$/CO ratio.

RWGS, the FT production increases even more because $CO_2$ is converted to CO. An additional FT production increase of about 2.3 tonne/h is possible by adding the hydrogen to the RWGS reactor. The amount of added hydrogen is also increased. Since an under-stoichiometric gas is fed to the FT reactors, some spare hydrogen is needed to makeup for the deficient hydrogen between the FT stages. That is why we cannot feed all the hydrogen to the RWGS reactor. Fig. 11 shows the effect of total hydrogen added on the FT production, which is nearly a linear relationship.

The main purpose of the acid gas removal unit is to remove $H_2S$ because of its poisonous effect on FT catalysts. By using an absorption type process, some $CO_2$ is unavoidably extracted as well. The effect of $CO_2$ extraction in the acid gas removal unit on FT production and hydrogen addition is shown in Fig. 12. Since the $H_2S$ concentration is approximately 200 ppm prior to the acid gas removal unit, it may be feasible to only use solid beds to adsorb and react $H_2S$ to lower the concentration to ppb levels. In that case, no $CO_2$ will be extracted and the production is increased by about 3 tonne/h compared to the case with 90% extraction. Detailed modeling and cost analysis is required to prove the feasibility of using adsorbent beds instead of the Selexol process. Product distribution in FT stages in PBtL process is shown in Fig. 10. The results correspond to the sum of 'Heavy HC' and 'Light HC' streams for each FT stage in Fig. 3.

### 4.2. Process performance

The overall results for the BtL and PBtL concepts are shown in Table 3. Since one of the novel features of the proposed PBtL design is FT reactor staging, the results of PBtL with and without staging is also presented. In all cases, the FT reactor volume is such that the CO conversion is 55% per FT reactor. Furthermore, the $H_2$/CO ratios at the inlet of FT reactors are the same and equal to 2.05. This may not be the optimal value and will be subject for further optimization. Moreover, in all three cases, the amount of $H_2$ added to the RWGS reactor is such that the syngas will have the chosen $H_2$/CO ratio (i.e. 2.05) prior to the first FT rector. As can be seen from Table 3, both the carbon efficiency and the FT production are more than doubled in the PBtL concept compared with BtL. Carbon efficiency is defined as the proportion of the biomass carbon that ends up in FT products containing at least five carbon atoms.

Compared to the BtL, the $CO_2$ released per produced unit of FT products is 16 times lower for the staged PBtL process. The extra production of fuel with the PBtL concept requires approximately 11.6 kWh electrical power per liter syncrude ($C_{5+}$). The density of syncrude ($C_{5+}$) is assumed to be 800 kg/m$^3$.

Both for the BtL and the one-stage PBtL, the tail gas stream contains large volumes of unconverted $H_2$ and CO. Therefore, it is possible to partly recycle it directly to the FT reactor. Here, 80% of the tail gas is chosen to be recycled to the FT reactor. This is a nominal value and will be subject to further optimization. For the BtL the amount of purge is set to 7% of the tail gas, while for the PBtL it is adjusted so that enough heat is available in the fired heater to heat up the steam to 850 °C prior to the SOEC; resulting 8.8% and 1.5% tail gas purge in the three and one stage case, respectively.

The overall results for the staged and one stage PBtL concepts are more or less similar. There is no dramatic increase in FT reactor volume, but the total amount of recycled gas is about 6.6 times larger in the one stage PBtL concept. As the $H_2$/CO ratios at the inlet of FT

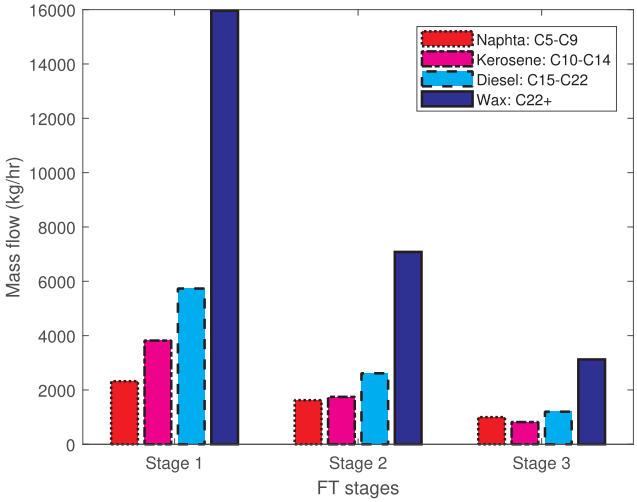


**Fig. 10.** Product distribution in FT stages in PBtL process. The results correspond to the sum of 'Heavy HC' and 'Light HC' streams for each FT stage in Fig. 3.

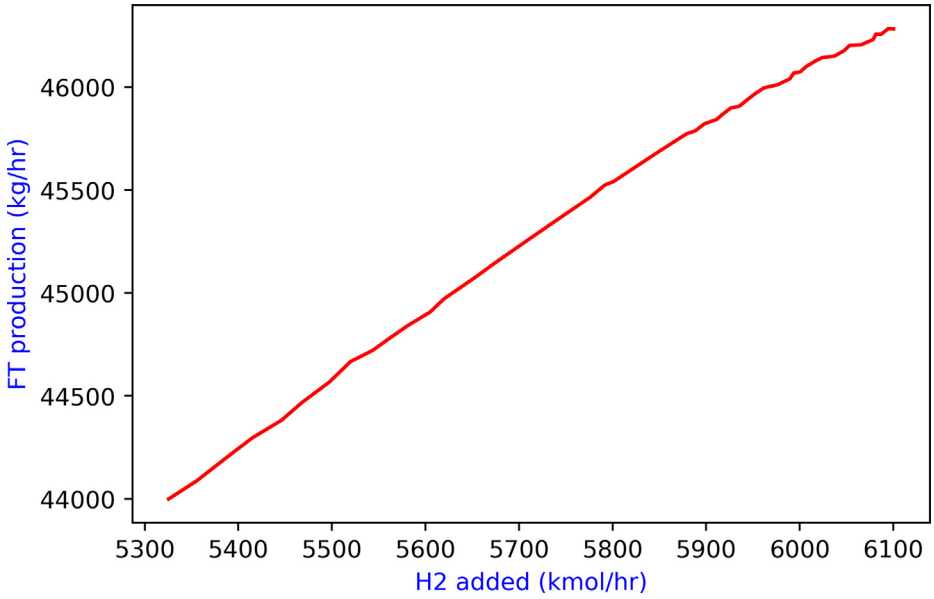


**Fig. 11.** Effect of total added hydrogen in PBtL process.

reactors are close to the stoichiometric consumption ratio, the ratios will not change much through the reactors. This implies that only small amounts of hydrogen is needed for makeup between the stages in staged PBtL concept, in order to maintain the same $H_2$/CO ratio for all stages. However, it is believed that there is a potential to improve the staged PBtl concept by optimizing the $H_2$/CO ratios.

Carbon flows within the BtL and staged PBtL concepts are shown in Figs. 13 and 14, respectively. For the BtL process, about 57% of the biomass carbon ends up as $CO_2$, which is removed in the syngas cleaning step. The main reason for the low carbon efficiency of the BtL process is that a substantial amount of CO is shifted to $CO_2$ in the WGS reactor. In the staged PBtL concept, however, the amount of carbon loss is reduced to about 7%. While, for the BtL concept, 38% of the carbon ends up in products, the figure is 91% for the PBtL concept. Due to the low once-through conversion, the recycle flow of the BtL process is four times larger than for the PBtL. Compared to the PBtL, the $CO_2$ concentration of the BtL recycle stream is 10 times higher.

The carbon flow is an important process descriptor, but the energy flow is even more revealing. The energy flow in the BtL and staged PBtL concepts are shown in Figs. 15 and 16, respectively. By assuming the specific power required for $O_2$ production in an air separation unit to be 0.4 kWh/kg $O_2$, electric power equivalent to about 4.4% of the LHV of the biomass is required in the BtL case. For the BtL case, the energy content of FT product is 53% of the LHV of the inlet biomass. In the staged PBtL case, the energy content of the products is equal to 128% of the biomass energy.

To get a better picture of the amount of heating and cooling required in the PBtL process, the energy composite curve is shown in Fig. 17. According to this figure, about 255 MW of excess heat mainly below 200 °C is available in the process which can be utilized to produce power and hydrogen. The horizontal hot line at 210 °C represents the steam generated during cooling of the FT reactors. Moreover, there is no need for any external heating, as there is enough heat within the process.

### 4.3. Increasing the energy efficiency by heating the SOEC

The PBtL model here accounts for an SOEC that operates at the thermoneutral potential, as explained in Section 3.4. In this mode, the electric energy need is equal to the enthalpy need, which is around

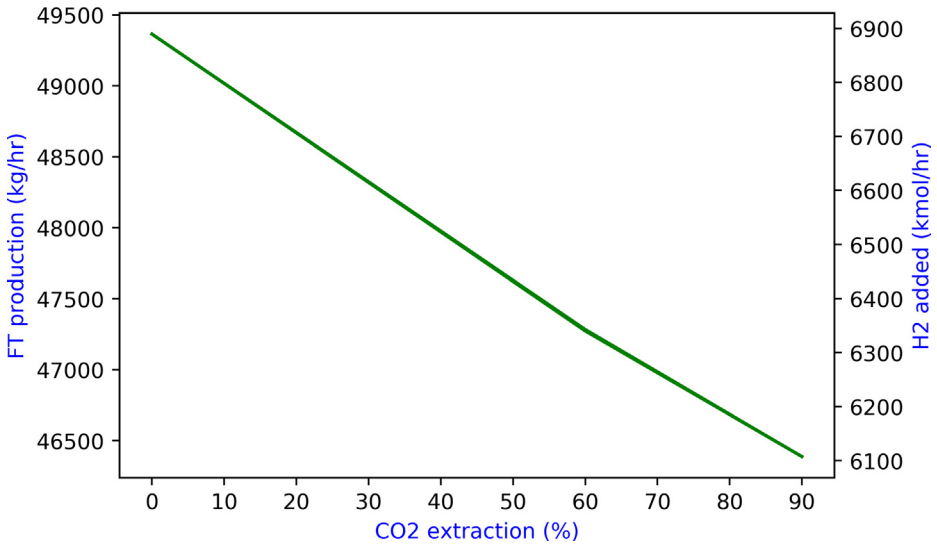


**Fig. 12.** Effect of $CO_2$ extraction in acid gas removal unit on FT production and hydrogen addition.

**Table 3**
Comparison of the BtL and PBtL concepts with 90% $CO_2$ extracted in acid gas removal unit.

| | BtL | PBtL | |
|---|---|---|---|
| | | Three FT stages | One FT stage |
| CO conversion in FT section per pass (%) | 55.0 | 90.9 | 55.1 |
| Carbon efficiency (overall) (%) | 37.8 | 91.3 | 91.0 |
| FT production (overall) (tonne/hr) | 19.2 | 46.4 | 46.2 |
| FT Reactor volume ($m^3$) | 297 | 645 | 700 |
| Required power in SOEC (MW) | – | 415.3 | 417.9 |
| Required power in ASU (MW) | 19.2 | – | – |
| Required power in Acid gas removal (MW) | 4.6 | 0.35 | 0.37 |
| $CO_2$ released (kg/L FT product) | 3.86 | 0.24 | 0.25 |
| Steam to SOEC (tonne/hr) | – | 137.0 | 137.8 |
| Steam to WGS (tonne/hr) | 11.0 | – | – |
| Recycle flow to the gasifier (tonne/hr) | 16.6 | 19.5 | 26 |
| Recycle flow to the FT reactor (tonne/hr) | 66.4 | 0 | 103.9 |
| Tail gas compositions (mol%) | | | |
| $H_2$ | 46.9 | 50.6 | 54.9 |
| CO | 25.4 | 25.5 | 30.6 |
| $CH_4$ | 5.3 | 12.7 | 8.2 |
| $CO_2$ | 17.9 | 1.8 | 1.3 |
| $N_2$ | 1.5 | 3.4 | 1.1 |

35 kWh $kg^{-1}_{H_2}$. The present SOEC model implemented in HYSYS is a one stage adiabatic cell model with a conversion of 80%. Furthermore, the extra fuel production with the PBtL process will require 11.6 $kWh_{el.}$ per liter syncrude. However, by feeding inlet steam at 850 °C and converting 20 mol% of the inlet steam, the electric energy requirement can be reduced from 35 to 29 kWh $kg^{-1}_{H_2}$, which in turn will lower the electric energy need to around 9.5 $kWh_{el.}$ per liter syncrude. This means that heat integrated SOEC in a PBtL takes residual biological $CO_2$, along with 9.5 $kWh_{el.}$ and convert it into a FT oil with an energy content of around 10 kWh/Liter.

This example considers a conversion of 20 mol%, not 80 as sought in the presented PBtL model. With a higher conversion over the SOEC, one will need much higher inlet temperature of the steam to obtain the same electric efficiency. How to realize this in detail belongs to more comprehensive studies, but somehow heat needs to be added to the SOEC and the simplest practical solutions are suggested here. In Table 4 the adiabatic cell operation is shown for 20 and 80 mol% conversion. The model input are the steam inlet steam temperature and the conversion rate (X) under adiabatic operation, as demonstrated in Section 3.4. It is clear that a 20 mol% conversion utilizes heat much better than a 80 mol% conversion. One approach is to stage the SOEC with interheating between the stages and where each stage is adiabatic and converts 20 mol% of the steam (0–0.2, reheat, 0.2–0.4, reheat, 0.4–0.6, etc.). Another approach is to recycle 80% of the SOEC product gas (0.8 $H_2$, 0.2 $H_2O$), add more steam, and heat this to 850 °C (now 0.6 $H_2$, 0.4 $H_2O$) and electrolyse this under the 20 mol% conversion (back to 0.8 $H_2$, 0.2 $H_2O$).

As neat as it seems to use waste heat for direct electricity reduction, this operation condition is not one that is commercially at present. Neither is operating an SOEC at 40 bar. It is a strong need for these two operating conditions still, from both practical and energetic points of view. The pressure challenge may simply be solved by placing the SOEC inside a pressure vessel, so that there is no pressure gradients from gases on the SOEC materials. The energy and temperature challenge of non-isothermal operation conditions, on the other hand, is a subject for a more detailed study. Here, as a first assessment of waste heat recovery, we suggest inlet steam and hydrogen at 850 °C and outlet temperatures of 650 °C, which is moderate temperature gradients. As an example solid oxide fuel cells of very similar materials as an SOEC are sold for flexible power production from natural gas, with an expectancy of cycling between room temperature and around 700 °C several times a week.

## 5. Economic analysis

### 5.1. Capital investment

Comparison of the total capital investment in million US dollars (M $) for the conventional BtL plant and the PBtL concept using one-stage and three-stage Fischer Tropsch system is shown in Table 5. The capital investment is here calculated from

$$C_{inv} = \left[\sum_i C_{PI,i}\right][1 + f_{land} + f_{site} + f_{building}][1 + f_{cont} + f_{eng}][1 + f_{dev} + f_{com}], \quad (25)$$

where $C_{PI,i}$ is the equipment purchase and installation cost, and $f_i$ represents additional cost factors for the project shown in Table 6 [49,50].

Equipment purchase and installation costs have been calculated using the base-cost method proposed by Guthrie-Ulrich [50], given by $C_{PI,i} = N_{t,i} C_{P_b,I_b}(I/I_b) f_P f_{mat} f_{inst} k_t^{N_{t,i}}$ where $C_{P_b,I_b}(S_k/N_{op,i})$ is the equipment purchase cost calculated as a function of the actual equipment size $S_k$ and the number of operating units $N_{op,i}$ at the cost index $I_b$ related to a reference year, $N_{t,i}$ is the total number of units per type of equipment, $I$ is the cost index for the actual year, $f_{mat}$ and $f_P = (P/P_b)^{k_P}$ are factors accounting for a different material and pressure than the one

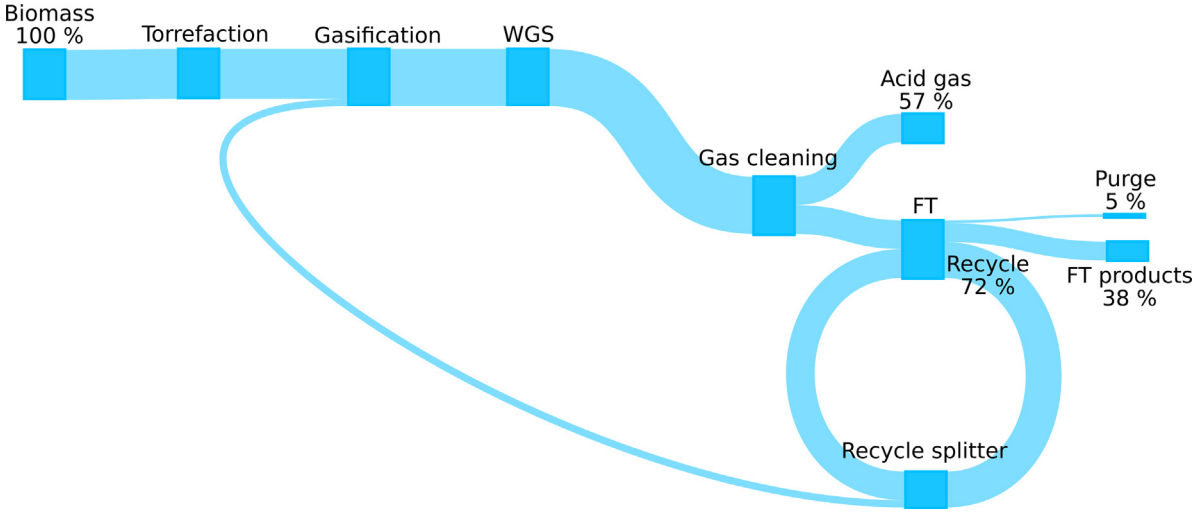


**Fig. 13.** Carbon flow of the BtL concept with 90% $CO_2$ extracted in acid gas removal unit.

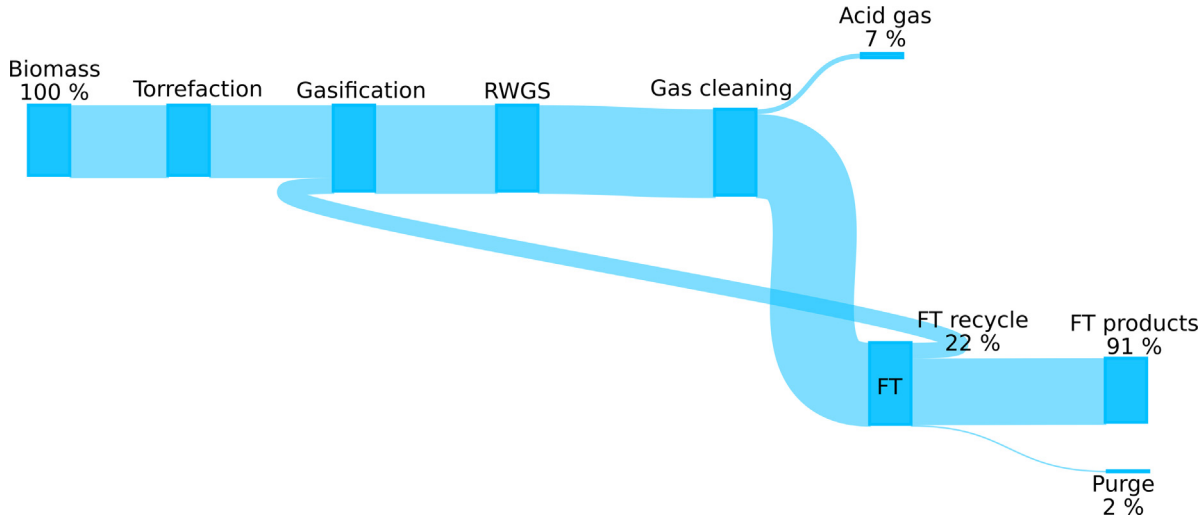


**Fig. 14.** Carbon flow of the staged PBtL concept with 90% $CO_2$ extracted in acid gas removal unit.

considered in the purchase cost function $C_{p,I_b}$, with $k_p$ being assumed to be constant and equal to 2.208. Further, $f_{inst,k}$ is the installation factor for each process equipment evaluated based on the methodology proposed by [51], and $k_t^{N_t}$ is the train cost factor where the parameter $k_t$ is assumed to be constant and equal to 0.9 [52,53]. The train cost factor accounts for cost reduction for multiple units due to share of auxiliaries and installation costs. All the equipment costs shown in Table 5 represent installed costs updated to 2017 based on the Chemical Engineering Plant Cost Index (CEPCI). Detailed information on the base cost functions and installation factors for all the equipment can be found in a previous publication by one of the authors [12]. The results shown in Table 5 assume the same plant capacity (435 $MW_{th}$ based on the LHV of dry biomass) and a unit installed cost for the SOEC of 1000 $/kW(el). The design of the EFG reactor for the BtL plant includes a radiation chamber for indirect quench of the syngas to 850 °C, which is replaced by the RWGS in the PBtL concept. The design of the Acid Gas Removal in the PBtL concept is designed as a one-stage Selexol system to remove the $H_2S$ content of the syngas. Despite the absence of the Air Separation Unit and the lower capital cost of the syngas conditioning, the capital investment for the PBtL concept becomes approximately 60% higher than for the conventional BtL plant. This is mainly due to the high capital cost of the SOEC technology, and the associated electric power supply, as well as the increased capacity of the FTS and the upgrading systems.

### 5.2. Operating costs and revenues

Comparison of the total annual operating cost and the annual revenues (M$) for the conventional BtL plant and the PBtL concept using one-stage and three-stage Fischer Tropsch system are shown in Tables 7 and 8. The annual operating cost for the plant is calculated from $C_{PROD} = C_F + C_{op,d} + C_{op,i} + C_{maint}$, where $C_F$ is the total cost of feed-stock supply, $C_{op,d}$ represents the variable direct operational cost dependent on the annual processing of feed-stock, $C_{op,i}$ are the fixed indirect operational costs required for having the plant in activity, and $C_{maint}$ are the maintenance costs. The total cost of feed-stock supply is calculated from $C_F = (M_F/\rho_F)\ t_{prod}\,[c_{pr} + c_{tr,f} + Lc_{tr,L}]$, where $M_F$ is the total mass flow rate of the raw feed-stock supplied to the plant, $t_{prod}$ denotes the annual production time, $\rho_F$ is the raw feed-stock density, $c_{pr}$ denotes the feed-stock production cost per unit volume and $c_{tr,f}$ and $c_{tr,L}$ are the fixed and distance-dependent transport costs per unit volume. The average feed-stock transport distance is here estimated from

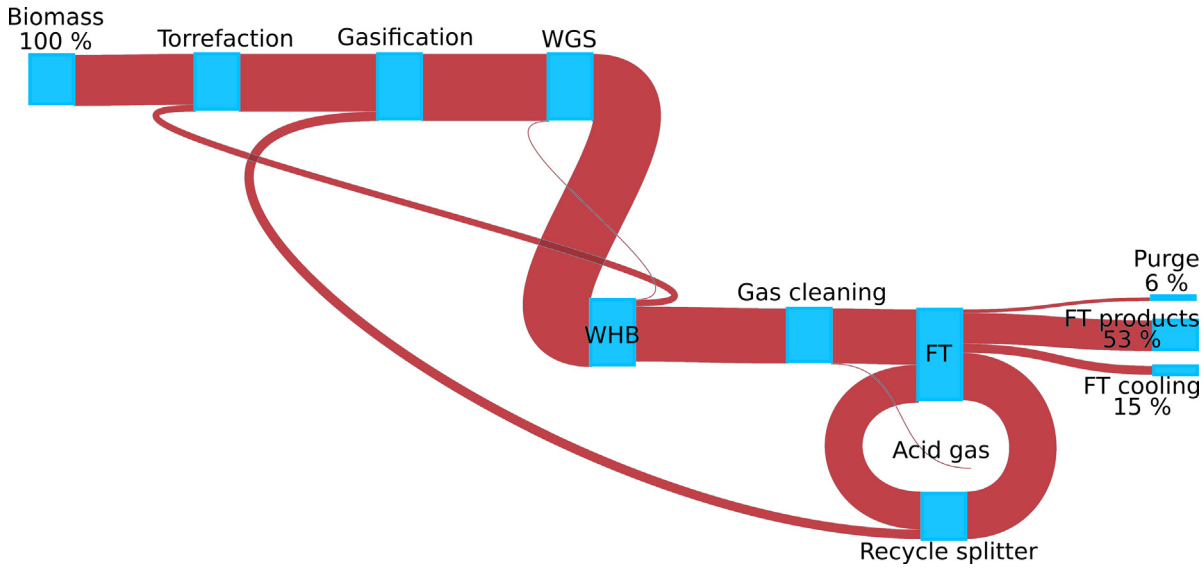


**Fig. 15.** Energy flow of the BtL concept. A substantial amount of energy required for acid gas cleaning is not shown in this diagram. The steam produced from the FT reactors (FT cooling) is energy that partly can be utilized.

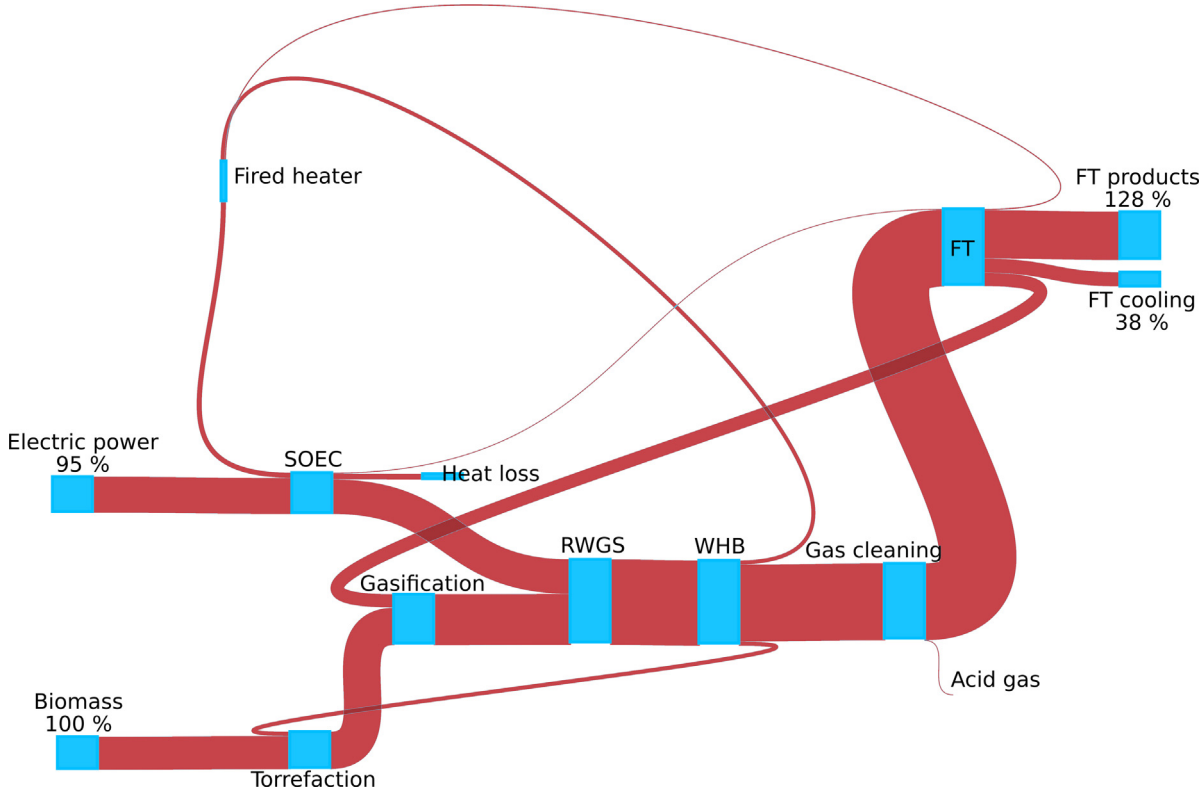


**Fig. 16.** Energy flow of the staged PBtL concept. The steam produced from the FT reactors (FT cooling) is energy that partly can be utilized.

$L = 2(M_F t_{prod}/m_{F,S})^{1/2}$ where $m_{F,S}$ is the feed-stock availability per unit area. The calculations shown in Table 7 assume 7800 h of annual operating time for the plant and values for $\rho_F$, $m_{F,S}$, $c_{tr,f}$ and $c_{tr,L}$, respectively, equal to 0.4 ton/m$^3$, 10 ton/ha, 7800 h, 2.4 \$/m$^3$ and 0.06 \$/m$^3$ km [54]. Direct operating costs associated with consumables and utilities as well as the revenues from products and by-products are calculated using the material flow rates obtained from the HYSYS simulations and the unit costs given in Tables 7 and 8. These results show that the total operating cost for the PBtL concept increases significantly, by a factor of 2.3, relative to the BtL plant due to the cost of electricity consumed by the SOEC. However, the increase in the operating cost is compensated by the increase in revenues from the naphtha, diesel and kerosene.

### 5.3. Cost of diesel and jetfuel

The levelized production cost of diesel and kerosene jetfuel, respectively denoted by $C_{bf}$ and $C_{jf}$, are defined as the average market prices per unit energy produced required so that the overall net present value (NPV) of the plant over its lifetime becomes zero. It is calculated

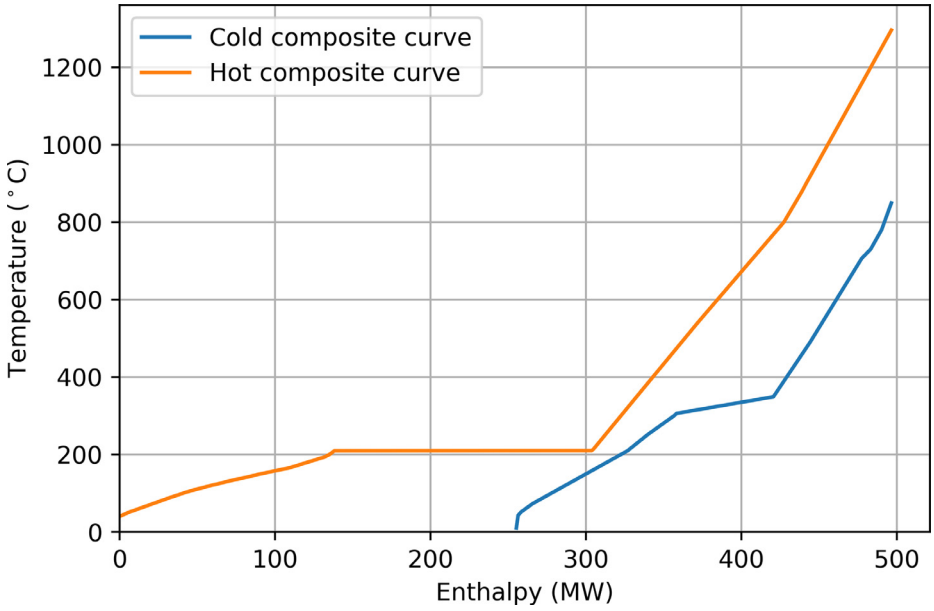


**Fig. 17.** Composite curves for the staged PBtL process.

**Table 4**
Temperature in and about along with electric work needed in the SOEC.

| | $X = 0.2$ | | $X = 0.8$ | |
|---|---|---|---|---|
| $T_{in}$/°C | $T_{out}$/°C | $w_{el}$/kWh $kg_{H_2}^{-1}$ | $T_{out}$ °C | $w_{el}$ kWh $kg_{H_2}^{-1}$ |
| 1100 | 825 | 26.2 | 602 | 30.8 |
| 1050 | 780 | 26.8 | 595 | 31.0 |
| 1000 | 740 | 27.2 | 592 | 31.4 |
| 950 | 710 | 27.7 | 587 | 31.7 |
| 900 | 680 | 28.2 | 586 | 32.1 |
| 850 | 650 | 28.8 | 582 | 32.4 |
| 800 | 625 | 29.8 | 578 | 33.0 |

**Table 5**
Comparison of the capital investment (M$) for the conventional BtL plant and the PBtL concepts using 1-stage and 3-stage Fischer Tropsch systems. It is assumed a plant capacity of 435 $MW_{th}$ based on the LHV of dry biomass and an installed cost of 1000 $/kW(el) for the SOEC.

| Capital investment | BtL | PBtL | |
|---|---|---|---|
| | | Three FT stages | One FT stage |
| EF gasification reactor and Reversed water gas shift | 254.9 | 253.7 | 260.0 |
| Slag quench and disposal | 5.5 | 5.5 | 5.5 |
| Air separation unit | 57.0 | – | – |
| Waste heat boiler and BFW system | 47.4 | 37.5 | 39.3 |
| Cyclone and water washer | 8.1 | 8.2 | 8.4 |
| WGS and COS hydrolysis | 33.2 | 1.8 | 1.8 |
| Acid gas removal (Selexol) | 52.3 | 5.2 | 5.3 |
| Sulfur separation and recovery | 0.3 | 0.3 | 0.3 |
| SOEC system | – | 391.6 | 394.0 |
| Cooling and compression of excess $O_2$ system | – | 25.6 | 25.1 |
| Fischer Tropsch system | 123.0 | 229.7 | 232.1 |
| Upgrading | 41.0 | 76.6 | 76.4 |
| Product storage | 8.2 | 15.3 | 15.2 |
| Waste water system | 24.1 | 30.2 | 31.0 |
| Chemicals (Initial batch) | 12.6 | 16.8 | 21.9 |
| Electrical system | 4.8 | 48.6 | 48.9 |
| Instrumentation and Control system | 33.8 | 52.5 | 53.1 |
| Land and site preparation | 235.6 | 366.5 | 370.7 |
| Foundation and Buildings | 78.5 | 122.2 | 123.6 |
| Plant Engineering | 109.9 | 171.1 | 173.0 |
| Contingency | 219.9 | 342.1 | 346.0 |
| Project development and licenses | 42.9 | 66.7 | 67.5 |
| Commissioning | 142.9 | 222.4 | 224.8 |
| Total | 1660.3 | 2626.5 | 2656.0 |

**Table 6**
Values for the capital investment cost factors in Eq. (25) that have been considered in the economic analysis.

| Capital cost factor | Value |
|---|---|
| Site preparation $f_{site}$ | 0.2 |
| Buildings, $f_{building}$ | 0.1 |
| Land, $f_{land}$ | 0.1 |
| Contingency, $f_{cont}$ | 0.2 |
| Plant Engineering, $f_{eng}$ | 0.1 |
| Project development and licenses, $f_{dev}$ | 0.03 |
| Commissioning, $f_{com}$ | 0.1 |

from

$$C_{bf} = \sum_{i=1}^{N} [(1+r)^{-i}(C_{TPI,i} + C_{PROD,i} - C_{INC,i}) \Big/ \sum_{i=1}^{N} [(1+r)^{-i} t_{prod,i}(H_{bf,i} + p_{jf} H_{jf,i})] \quad (26)$$

**Table 7**
Comparison of the annual operating costs (M$) for the conventional BtL plant and the PBtL concepts using one-stage and three-stage Fischer Tropsch systems.

| Operating cost | Assumptions | BtL | PBtL | |
|---|---|---|---|---|
| | | | Three FT stages | One FT stage |
| Feed-stock supply | – | 48.9 | 48.9 | 48.9 |
| Chemicals | See note[a] | 6.62 | 12.60 | 12.84 |
| Fresh water | 0.49 $/$m^3$ [55] | 0.09 | 0.08 | 0.10 |
| Process water | 8.34 $/$m^3$ [55] | 7.27 | 10.01 | 10.38 |
| Filter residue disposal | 40 $/ton [55] | 3.27 | 3.27 | 3.27 |
| Electricity | 0.05 $/kWh | 16.23 | 163.56 | 164.46 |
| Labor | See note[b] | 5.46 | 8.48 | 8.58 |
| Maintenance | 2% $C_{PI}$ | 15.71 | 24.40 | 24.69 |
| Insurance and taxes | 2% $C_{INV}$ | 33.21 | 52.50 | 53.11 |
| Administration and Services | 1% $C_{INV}$ | 16.60 | 26.25 | 26.56 |
| Emissions | 7.24 $/ton | 2.85 | 0.21 | 0.22 |

[a] Unit prices for consumables: 110 $/kg for FTS catalyst (Cobalt based) [10], 90 $/kg for both hydrotreating and hydrocracking catalyst, 5.3 $/liter for Selexol [56], 65 $/kg for ZnO, 17.3 $/liter for WGS catalyst [10], 25 $/kg for COS hydrolysis catalyst.

[b] One plant manager at 161.7 k$/year, one operation and maintenance manager at 88.2 k$/year, two plant engineer at 95 k$/year, 7 maintenance technician 17 shift operator at 58.8 k$/year, 3 shift supervisor at 66.2 k$/year, two administration and 7 site/building maintenance at 36.8 k$/year. 30% labor burden, 30% overhead with 1.3 overhead cost factor.

**Table 8**
Comparison of the annual revenue (M$) for the conventional BtL plant and the PBtL concepts using one-stage and three-stage Fischer Tropsch systems, based on current market values for diesel and jetfuel equal to 0.8 and 1.26 $/liter.

| Revenues | Assumptions | BtL | PBtL | |
|---|---|---|---|---|
| | | | Three FT stages | One FT stage |
| Jet fuel | 1.26 $/liter [57] | 25.41 | 62.28 | 61.86 |
| Diesel | 0.8 $/liter [57] | 97.37 | 238.66 | 237.07 |
| Naphtha | 0.31 $/liter [57] | 10.05 | 24.62 | 24.46 |
| LPG | 0.18 $/liter [57] | 5.63 | 16.59 | 19.37 |
| Heat | 16.7 $/MWh [58] | 31.58 | 21.33 | 23.12 |
| Slag[a] | 20 $/ton[a] | 0.03 | 0.03 | 0.03 |
| Sulfur | 100 $/ton | 0.05 | 0.05 | 0.05 |

[a] It has been assumed that the slag from EFG can be sold as agglomerate with a market price of 20 $/ton.

and $C_{jf} = p_{jf} C_{bf}$, where $r$ is the expected return of investment, $C_{INV,i}$, $C_{OP,i}$, $C_{REV,i}$, $H_{bf,i}$ and $H_{jf,i}$ are, respectively, the distribution of the capital investment, the annual operating costs, the annual income from co-products and the annual energy production of diesel and kerosene jet fuel over the life time of the plant. The parameter $p_{jf}$ represent the market price of kerosene jet fuel relative to diesel, here assumed to be constant and equal to 1.6. The financial assumptions considered for evaluating Eq. (26) are shown in Table 9. Fig. 18 compares the variation of the levelized cost of biodiesel as a function of the electricity price for the conventional BtL plant and for the PBtL plant concept with 1 and 3-stage FTS based on a unit installed cost of the SOEC equal to 500, 1000 and 2000 $/kW(el). This range for the cost of the SOEC has been considered to be achievable [59] for large-scale commercial deployment in a short, medium and long term perspective. Here it is assumed that the SOEC stacks are replaced every 5 years, which correspond to a maintenance cost of 20% of the total installed cost for the SOEC. The blue and green regions in Fig. 18 indicates representative ranges of the levelized cost of electricity that can be achieved by onshore wind and solar photo-voltaic technologies in the time-frame between 2017 and 2050 [60]. The results shown in Fig. 18 indicates that the economic performance of the PBtL concept is very sensitive to the

**Table 9**
Financial assumptions considered to calculate the levelized cost of diesel and kerosene jet fuel.

| Financial parameter | Value/assumption |
|---|---|
| Plant life time | 25 years |
| Debt equity ratio | 70–30 |
| Depreciation | linear |
| Construction and commissioning period | 3 year |
| Capital distribution during construction and commissioning | year 1: 30%/ year 2: 50%/year 3: 20% |
| Return of Investment | 10% |
| Loan repayment period | 10 years |
| Loan Interest rate | 7% |

price of electricity. When the cost of the SOEC is above approximately 2000 $/kW(el), the cost of biodiesel produced by the PBtL concept is below the cost achieved by the conventional BtL for price of electricity below 0.1 $/kWh. For a more realistic scenario where the installed cost of the SOEC system becomes 1000 $/kW(el) and the electricity price is 0.05 $/kW(el) (current market price in Norway), the cost of biodiesel produced from the PBtL concept is 1.7 $/liter, approximately 30% lower than the production cost achieved by the conventional BtL plant. For this cost of the SOEC and considering zero cost for the electricity, the cost of biodiesel produced by the PBtL concept can reach 1.2 $/liter. This value is in line with current market prices for fossil diesel. In a long-term perspective, if the cost of SOEC is reduced by 50%, to 500 $/kW(el), the impact on the biofuel production cost achieved by the PBtL concept can be reduced by approximately 15% reaching a production cost close to 1.1 $/liter. Break-even prices of electricity which makes the biofuel production cost for the conventional BtL and the PBtL process to be equal is 0.1, 0.13 and 0.18 $/kWh based an installed cost of the SOEC equal to 2000, 1000 and 500 $/kW(el) respectively.

Fig. 19 compares the contribution from main items in the capital investment, the operating costs and the revenues from co-products to the cost of biodiesel obtained by the conventional BtL plant and the PBtL plant concept for an installed cost of the SOEC and an electricity price equal to 1000 $/kW(el) and 0.05 $/kWh(el), respectively. For the BtL plant, both the feed-stock supply cost and the capital investment in the gasification and syngas conditioning contribute approximately a 35% of the total biodiesel production cost. For the PBtL concept, the cost of electricity and the SOEC become the main contributors with approximately 40% of the cost of biodiesel.

## 6. Discussion

The present analysis of producing liquid fuel from biomass with added hydrogen from water splitting is based on a few key learnings from literature. First, adding hydrogen is a necessity for high carbon efficiency. A high carbon efficiency means a more efficient production in terms of process equipment utilization, but more importantly, a proportionally lower amount of biomass harvesting is needed for a given fuel production. Second, splitting of water can be conducted by several thermochemical, electrochemical or catalytic means; nevertheless, employing high temperature electrolysis of steam seems particularly advantageous. Admittedly, this potential advantage depends on the electrical power supply situation at the production site, obviously the price, but also to what extent the power is based on a high proportion of renewable energy. It is also a learning that using an entrained flow gasifier at high temperature gives an overall benefit in terms of gas composition, gas cleaning and overall energy efficiency. At last, production of renewable fuel is favorably done through Fischer-Tropsch synthesis, particularly when jet fuel is one of the targeted products.

With these constraints, we have analyzed PBtL in further detail and compared with BtL, that is with no extra hydrogen available. The developed PBtL flowsheet contains a few key elements that are different from a conventional BtL or FT plant. The reverse water gas shift reaction utilizes the high temperature of the entrained flow gasifier to convert $CO_2$ to CO, with added hydrogen, and thereby fulfilling the high carbon efficiency target. Integrating RWGS with the EF gasifier has the important additional benefit of chemically quenching the produced syngas to a temperature where further cooling can be performed by a conventional steel based water boiler. Thus, there is ample steam available for feeding a high temperature SOEC electrolysis cell. For high efficiency of the SOEC, it has been shown that further heating of the steam reduces power consumption and facilitates isothermal operation with low ohmic losses. Such heating is conveniently performed in a

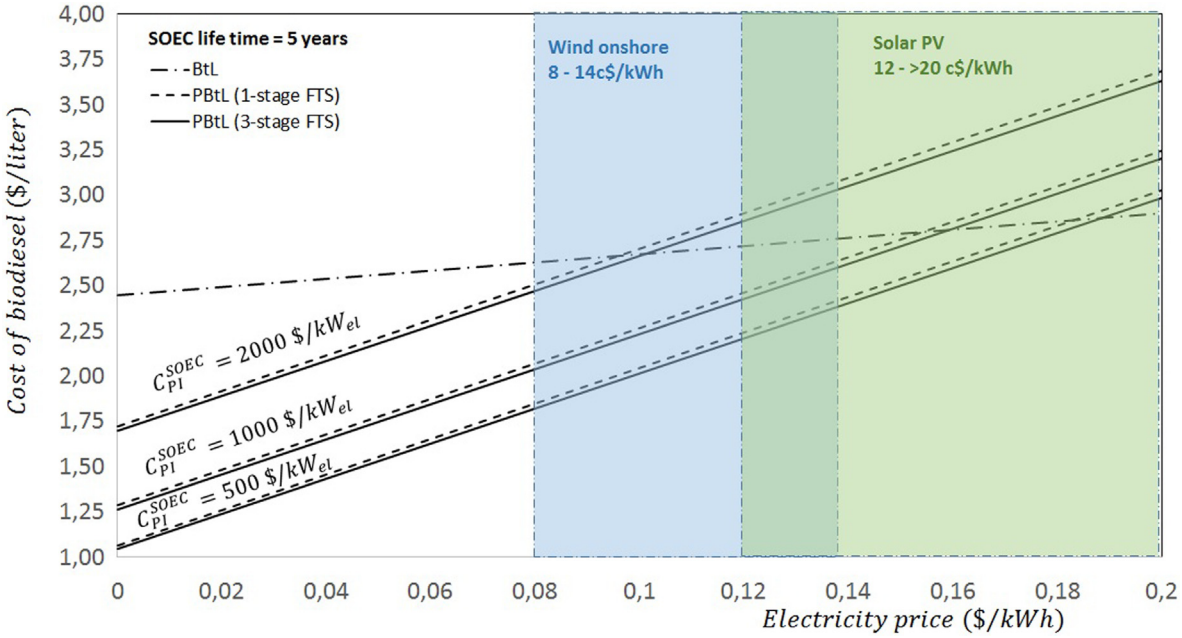


**Fig. 18.** Variation of the levelized cost of biodiesel as a function of the electricity price for the conventional BtL plant and for the PBtL plant concept with 1 and 3-stage FTS based on a unit installed cost of the SOEC equal to 500, 1000 and 2000 $/kW(el). Comparison with electricity prices based on wind and solar power is for illustration purposes only and does not imply a specific preference for electricity supply to PBtL.

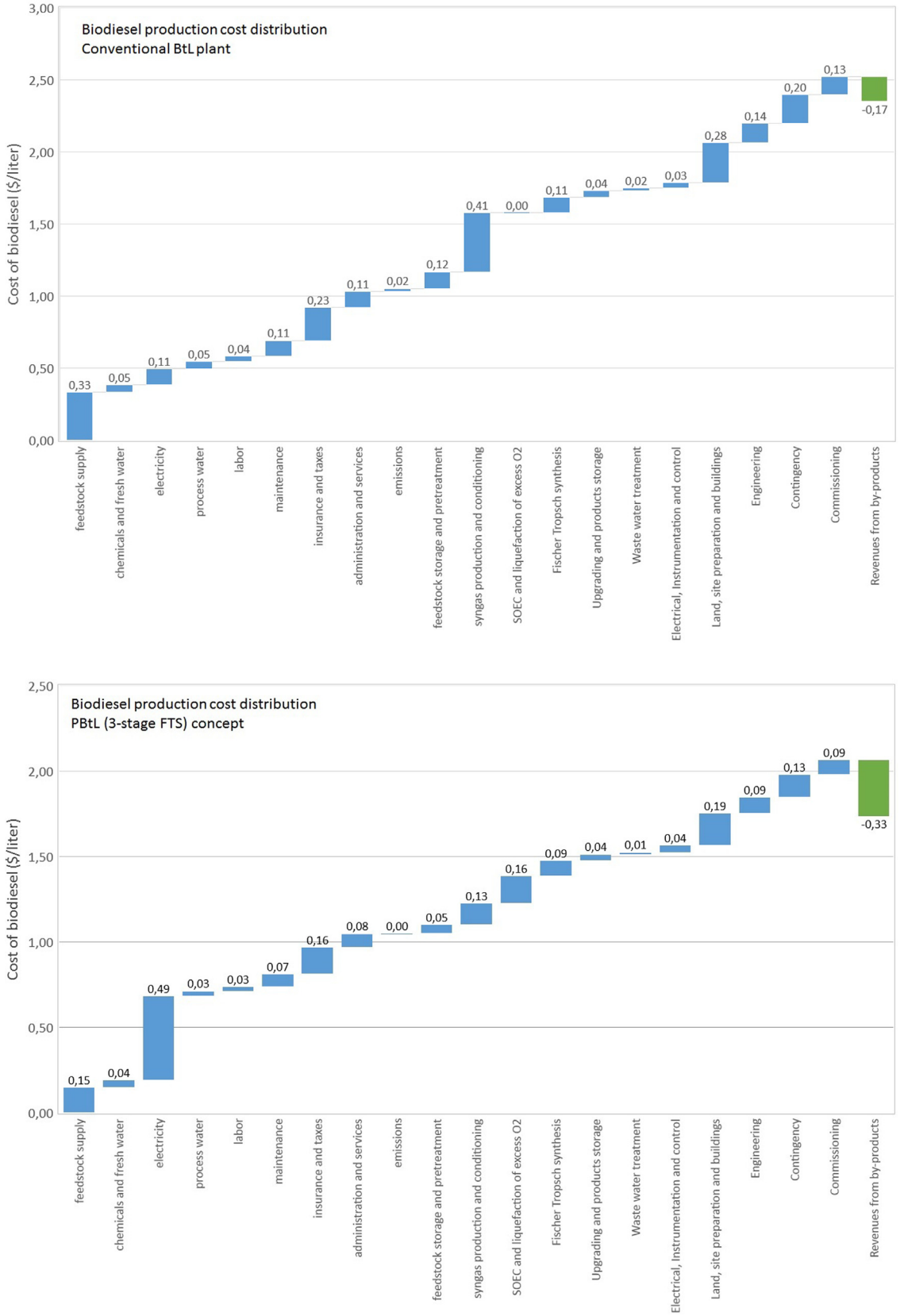


**Fig. 19.** Contribution from the main items in the capital investment, the operating costs and the revenues from co-products to the cost of biodiesel obtained by the conventional BtL plant (upper figure) and for the PBtL plant concept with 3-stage FTS (lower figure). The unit installed cost of the SOEC and the electricity price are assumed to be 1000 $/kW(el) and 0.045 $/kWh(el), respectively.

fired heater fueled with purge gas leaving the FT reactor(s). A certain amount of gas has to be purged in any case to avoid nitrogen in the biomass to be accumulated in the recycle loop of FT tail gas. The carbon that is combusted in this way amounts only to a 2–3% loss in carbon efficiency.

A key purpose of the present analyses has been to have a close look at the FT section with due consideration of maximizing product selectivity and yield. In particular, a suggested advantage of having staged FT-reactors has been simulated. Staged reactors, meaning a series of FT reactors, has the benefit of high once-through conversion as the conversion in a single reactor is constrained due to limitations in reactor size, catalytic robustness and heat removal. Hydrocarbons and water are withdrawn between the reactors. High conversion means less gas that needs to be recycled. Unconverted syngas, as well as $CO_2$, can be recycled to the gasifier or to the inlet of the FT reactor(s). As a first approximation, it was found beneficial to recycle all the tail gas to the gasifier for $CO_2$ conversion in case of staged reactors due to the high conversion and consequently small gas volumes. For a single FT reactor, however, most tail gas must be recycled to the front end of the FT section to secure hydrocarbon synthesis of large amounts of unconverted syngas.

A disadvantage of having only one synthesis reactor is that the recycle volumes are exceedingly high, increasing by a factor of almost 7. Having a series of three reactors will definitely add to costs, but might have operational benefits, e.g. during shut-downs and exchange of catalyst. Presently, we do not draw any conclusion as to which option for the FT synthesis reactor configuration is to be preferred.

As expected, there are substantial differences between conventional BtL and PBtL. The carbon efficiency is only 38% in the former case, increasing to 91% and beyond when hydrogen is added. The energy content in the FT products are 53% of dried biomass for BtL in contrast to an increase to 128% when hydrogen is incorporated. Note that a full energy efficiency calculation incorporating Pinch analysis, energy needed for biomass harvesting, transportation, drying and pretreatment has not been performed at this stage. On the other hand, there is a significant surplus of steam generated in the FT-reactors and during process gas cooling that can be used for biomass drying, pretreatment and optionally electricity production.

The analysis of hydrogen distribution between RWGS and FT reactors is conclusive in that all available hydrogen is to be used to shift $CO_2$ to CO. There is only a residual 4% hydrogen needed to readjust the $H_2$/CO ratio prior to the second and third FT reactor in the staged concept. In addition comes a few % needed in the upgrading section; this is not part of the present study. One might suspect that adding the first molecules of hydrogen are more effective than the last molecules. This is, in fact, hardly the case. There is an almost linear relationship between added hydrogen and extra hydrocarbons produced. The conclusion from this is that if it is beneficial from an economic point of view to add hydrogen, the full amount for maximum conversion of $CO_2$ should be added.

As a base case in the present work, it has been assumed that 90% of $CO_2$ in the raw syngas is removed in the acid gas removal section. Even though this high fraction of $CO_2$ is vented, the overall PBtL carbon efficiency is still above 90%. Depending on acid gas removal technology selection, the amount of vented $CO_2$ is a variable. The results are straight forward; the less $CO_2$ removed, the more carbon ends up in the FT-products and proportionally more hydrogen needs to be added.

Some comments are due the technology readiness level of the process units in the PBtL plant. There are three technologies that need further attention in terms of feasibility, optimization and scale-up. RWGS is a simple high-temperature reaction. Gas phase kinetic simulations show, however, that the residence time needed for equilibration can be exceedingly long giving high reactor volumes. The effect of a simple catalyst like a porous alumina should be investigated. Entrained flow-gasifiers are well-known for gasification of coal, and demonstration units have been operated on biomass. Still, operational experience with biomass in limited. One challenge that has been expressed is control of the slag formation and avoiding solidification and blockage at the exit. As to SOEC, no large installation is known, although ample laboratory and pilot work has proven the principle. A few companies supply, or are ready to supply, SOEC units, but not for operation at the desired conditions of 40 bar and 1000 °C. Degradation of the membrane oxide with time, requiring steady increase in temperature, limits the life-time to ca. 3 years at a nominal temperature of 700–800 °C. Produced oxygen is flushed out of these units with nitrogen or steam, and use of hot oxygen must be regarded as unproven technology.

## 7. Conclusions

The present work has demonstrated the potential benefits of introducing renewable power to the biomass to liquid process. The following main observations can be drawn from this study:

- By adding hydrogen, produced from renewable electric power, to the BtL process, the carbon efficiency can be increased from 38% to more than 90%. The increased carbon efficiency is possible because the water gas shift reaction is avoided and instead a reversed water gas shift is introduced to convert $CO_2$ to CO.
- Because of the increased carbon efficiency, the total fuels production rate of the PBtL can be increased by a factor of 2.4 compared to a conventional BtL with same amount of biomass feed. Even for different syntheses, this production increase is comparable to the findings of Hannula [5]. In addition, the emitted amount of $CO_2$ per produced unit can be reduced by a factor of 16.
- Based on detailed process simulation models and cost models, the PBtL process is found to be more profitable than a conventional BtL process for realistic power prices. With an electrical power price of 0.05 $/kWh and an SOEC investment cost of 1000 $/kW(el) installed, the levelized cost of producing advanced biofuel with the PBtL process is 1.7 $/liter, which is approximately 30% lower that for the conventional BtL. The levelized cost sensitivities of the power price and the investment cost are shown in Fig. 18.
- There is a near linear relationship between added hydrogen and production of surplus FT-products, meaning that maximum hydrogen addition is favorable.
- For each extra liter of syncrude ($C_{5+}$) produced by adding hydrogen, 11–12 kWh electric power is required. By heat integrating the SOEC with the plant for iso-thermal operation, the electric power needed can be lowered to 9–10 kWh per liter of extra fuel. This is approximately the energy content of diesel. However, this target may be difficult to reach, but a reduction should be possible.
- All hydrogen should be added to the RWGS except the amount needed for makeup of the $H_2$/CO ratio between stages.
- An entrained flow gasifier is perfectly suited for enhanced carbon efficiency by adding a section for chemical quenching of $CO_2$.
- Selection of acid gas removal technology is only governed by the need for sulfur cleaning. As little $CO_2$ as possible should accompany the captured sulfur.
- There are significant amounts of excess heat generated during FT synthesis and cooling of process gases that can be used for biomass drying, pretreatment, power and hydrogen production.

Most of the elements of the proposed process are mature and proven technology, but there are elements that are less proven. There are also aspect of the proposed concept that can be improved. In order to make the PBtL process concept more profitable some further work will be pursued.

- As already stated, the heat integration with the SOEC may increase the electrical efficiency. Further work will include a design of the SOEC process that is heat integrated with the rest of the plant.
- In addition to the SOEC, an alternative process for generating

hydrogen from low temperature heat will be considered.
- RWGS technology should be investigated at the present conditions of 900–1100 °C, particularly the potential need for a catalyst.
- Alternative kinetic models of the FT synthesis including selectivity models will be evaluated. The models will be validated against new laboratory data.
- The optimal $H_2$/CO ratios to the FT reactors and the optimal staging of the FT reactor path will be generated based on a systematic method [8].
- It may be feasible with a solid adsorption process like ZnO or $CuCO_3$ to remove sufficient amount of $H_2S$. But the cost of this process should be compared to absorbent processes like Selexol and methanol.

## Acknowledgements

The Research Council of Norway (project No. 267989) is greatly acknowledged for the financial aid of this project.

## References

[1] Carbon offsetting scheme for international aviation corsia. http://www.iata.org/policy/environment/Pages/corsia.aspx.
[2] Rytter E, Ochoa-Fernandez E, Fahmi A. Biomass-to-liquids by the Fischer-Tropsch process. In: Imhof P, van der Waal J-K, editors. Catalytic process development for renewable materials. New York: Wiley; 2013. p. 265–308. [Ch. 12].
[3] Agrawal R, Singh NR, Ribeiro FH, Delgass WN. Sustainable fuel for the transportation sector. Proc Natl Acad Sci 2007;104(12):4828–33. https://doi.org/10.1073/pnas.0609921104. arXiv:http://www.pnas.org/content/104/12/4828.full.pdf, URL http://www.pnas.org/content/104/12/4828.abstract.
[4] Bernical Q, Joulia X, Noirot-Le Borgne I, Floquet P, Baurens P, Boissonnet G. Sustainability assessment of an integrated high temperature steam electrolysis-enhanced biomass to liquid fuel process. Ind Eng Chem Res 2013;52(22):7189–95. https://doi.org/10.1021/ie302490y.
[5] Hannula I. Hydrogen enhancement potential of synthetic biofuels manufacture in the European context: a techno-economic assessment. Energy 2016;104:199–212. https://doi.org/10.1016/j.energy.2016.03.119.
[6] Dietrich R-U, Albrecht FG, Maier S, König DH, Estelmann S, Adelung S, et al. Cost calculations for three different approaches of biofuel production using biomass, electricity and $CO_2$. Biomass Bioenergy 2017:1–9. https://doi.org/10.1016/j.biombioe.2017.07.006. URL http://linkinghub.elsevier.com/retrieve/pii/S0961953417302271.
[7] Rytter E. Gas to liquids plant with consecutive fischer-tropsch reactors and hydrogen make-up. US Patent App. 12/515,933 (Jun. 3 2010). URL https://www.google.com/patents/US20100137458.
[8] Hillestad M. Systematic staging in chemical reactor design. Chem Eng Sci 2010;65(10):3301–12. https://doi.org/10.1016/j.ces.2010.02.021.
[9] Sims RE, Mabee W, Saddler JN, Taylor M. An overview of second generation biofuel technologies. Bioresour Technol 2010;101(6):1570–80. https://doi.org/10.1016/j.biortech.2009.11.046.
[10] Swanson RM, Satrio JA, Brown RC, Hsu DD. Techno-economic analysis of biofuels production based on gasification techno-economic analysis of biofuels production based on gasification Alexandru Platon. Energy 2010;89:S11–9. https://doi.org/10.1016/j.fuel.2010.07.027. URL http://linkinghub.elsevier.com/retrieve/pii/S0016236110003741.
[11] Hunpinyo P, Narataruksa P, Tungkamani S, Pana-Suppamassadu K, Chollacoop N. Evaluation of techno-economic feasibility biomass-to-energy by using ASPEN Plus: a case study of Thailand. Energy Procedia 2013;42:640–9. https://doi.org/10.1016/j.egypro.2013.11.066.
[12] Kempegowda RS, Del Alamo G, Berstad D, Bugge M, Matas Güell B, Tran KQ. CHP-integrated fischer-tropsch biocrude production under norwegian conditions: techno-economic analysis. Energy Fuels 2015;29(2):808–22. https://doi.org/10.1021/ef502326g.
[13] Del Alamo G, Kempegowda RS, Skreiberg Ø, Khalil R. Decentralized production of Fischer-Tropsch biocrude via coprocessing of woody biomass and wet organic waste in entrained flow gasification: techno-economic analysis. Energy Fuels 2017;31(6):6089–108. https://doi.org/10.1021/acs.energyfuels.7b00273.
[14] Qin K, Jensen PA, Lin W, Jensen AD. Biomass gasification behavior in an entrained flow reactor: gas product distribution and soot formation. Energy Fuels 2012;26(9):5992–6002. https://doi.org/10.1021/ef300960x.
[15] Zhou J, Chen Q, Zhao H, Cao X, Mei Q, Luo Z, Cen K. Biomass-oxygen gasification in a high-temperature entrained-flow gasifier. Biotechnol Adv 2009;27(5):606–11. https://doi.org/10.1016/j.biotechadv.2009.04.011.
[16] Hernández JJ, Aranda-Almansa G, Bula A. Gasification of biomass wastes in an entrained flow gasifier: effect of the particle size and the residence time. Fuel Process Technol 2010;91(6):681–92. https://doi.org/10.1016/j.fuproc.2010.01.018.
[17] Phanphanich M, Mani S. Impact of torrefaction on the grindability and fuel characteristics of forest biomass. Bioresour Technol 2011;102(2):1246–53. https://doi.org/10.1016/j.biortech.2010.08.028.
[18] Arias B, Pevida C, Fermoso J, Plaza MG, Rubiera F, Pis JJ. Influence of torrefaction on the grindability and reactivity of woody biomass. Fuel Process Technol 2008;89(2):169–75. https://doi.org/10.1016/j.fuproc.2007.09.002.
[19] Wang L, Barta-Rajnai E, Skreiberg O, Khalil R, Czégény Z, Jakab E, et al. Impact of torrefaction on woody biomass properties. Energy Procedia 2017;105:1149–54. https://doi.org/10.1016/j.egypro.2017.03.486.
[20] Olanders B, Steenari BM. Characterization of ashes from wood and straw. Biomass Bioenergy 1995;8(2):105–15. https://doi.org/10.1016/0961-9534(95)00004-Q.
[21] Kremling M, Briesemeister L, Gaderer M, Fendt S, Spliethoff H. Oxygen-blown entrained flow gasification of biomass: impact of fuel parameters and oxygen stoichiometric ratio. Energy Fuels 2017;31(4):3949–59. https://doi.org/10.1021/acs.energyfuels.6b02949.
[22] Weiland F, Hedman H, Wiinikka H, Marklund M. Pressurized entrained flow gasification of pulverized biomass – experiences from pilot scale operation. Chem Eng Trans 2016;50:325–30. https://doi.org/10.3303/CET1650055.
[23] Arnold K, Stewart M, editors. Surface production operations: design of gas-handling systems and facilities 2nd ed.Woburn: Gulf Professional Publishing; 1999. https://doi.org/10.1016/B978-0-88415-822-6.50025-8. [link].URL https://www.sciencedirect.com/science/article/pii/B9780884158226500258.
[24] Chen C. A technical and economic assessment of $CO_2$ capture technology for igcc power plants [Ph.D. thesis]. Carnegie Mellon University; 2005.
[25] Doctor R, Molburg J, Thimmapuram P. KRW oxygen-blown gasification combined cycle: carbon dioxide recovery, transport, and disposal, 1996. doi:10.2172/373835. URL http://www.osti.gov/scitech/servlets/purl/373835.
[26] Tsunatu DY, Mohammed-Dabo IA, Waziri SM. Technical evaluation of selexol based $CO_2$ capture process for a cement plant. British J Environ Climate Change 2015;1(5):52–63. https://doi.org/10.9734/BJECC/2015/12482.
[27] Burheim OS. Engineering energy storage. 1st ed. Elsevier: Academic Press; 2017.
[28] Schulz H. Short history and present trends of Fischer-Tropsch synthesis. Appl Catal A: General 1999;186(1–2):3–12. https://doi.org/10.1016/S0926-860X(99)00160-X. URL http://linkinghub.elsevier.com/retrieve/pii/S0926860X9900160X.
[29] Rytter E, Holmen A. Perspectives on the effect of water in cobalt Fischer-Tropsch synthesis. ACS Catal 2017;7(8):5321–8. https://doi.org/10.1021/acscatal.7b01525.
[30] Rytter E, Holmen A. Deactivation and regeneration of commercial type Fischer-Tropsch co-catalysts a mini-review. Catalysts 2015;5(2):478–99. https://doi.org/10.3390/catal5020478. URL http://www.mdpi.com/2073-4344/5/2/478.
[31] Hamelinck CN, Faaij AP, den Uil H, Boerrigter H. Production of FT transportation fuels from biomass; technical options, process analysis and optimisation, and development potential. Energy 2004;29(11):1743–71. https://doi.org/10.1016/j.energy.2004.01.002.
[32] Van Bibber L, Shuster E, Haslbeck J, Rutkowski M, Olsen S, Kramer S. Baseline technical and economic assessment of a commercial scale Fischer-Tropsch liquids facility, DOE/NETL-2007/1260, National Energy Technology Laboratory, April 2007. https://edx.netl.doe.gov/storage/f/2016-09-29T15:07:09.436Z/DOE NETL 2007 1260.pdf.
[33] Bechtel. Baseline design/economics for advanced Fischer-Tropsch technology; 1998.
[34] Bechtel. Aspen process flowsheet simulation model of a biomass-based gasification, Fischer Tropsch liquefaction and combined-cycle power plant; 1998.
[35] Robinson PR, Dolbear GE. Chapter 7 Hydrotreating and hydrocracking: fundamentals hydroprocessing units: similarities and differences. Water 2004:177–218. https://doi.org/10.1007/978-0-387-25789-17. URL http://www.springerlink.com/index/x612423028646638.pdf.
[36] Amsterchem. URL http://www.AmsterChem.com.
[37] Burnham AK. Estimating the heat of formation of foodstuffs and biomass; 2010:1–11. URL https://e-reports-ext.llnl.gov/pdf/459155.pdf.
[38] Tapasvi D, Khalil R, Skreiberg Ø, Tran KQ, Grønli M. Torrefaction of Norwegian birch and spruce: an experimental study using macro-TGA. Energy Fuels 2012;26(8):5232–40. https://doi.org/10.1021/ef300993q.
[39] Govin A, Repelin V, Guyonnet R, Rolland M, Duplan J-L. Effect of torrefaction on grinding energy requirement for thin wood particle production. Récents Progrès en Génie des Procédés 2009;98(756):1–6.
[40] Gri-mech. URL http://www.me.berkeley.edu/gri-mech/.
[41] Cantera. URL http://www.cantera.org/docs/sphinx/html/index.html.
[42] Goodwin DG, Moffat HK, Speth RL. Cantera: an object-oriented software toolkit for chemical kinetics, thermodynamics, and transport processes, http://www.cantera.org, version 2.3.0; 2017. doi:10.5281/zenodo.170284.
[43] Todic B, Ma W, Jacobs G, Davis BH, Bukur DB. Effect of process conditions on the product distribution of Fischer Tropsch synthesis over a re-promoted cobalt-alumina catalyst using a stirred tank slurry reactor. J Catal 2014;311(Supplement C):325–38. https://doi.org/10.1016/j.jcat.2013.12.009. URL http://www.sciencedirect.com/science/article/pii/S0021951713004430.
[44] Hillestad M. Modeling the Fischer-Tropsch product distribution and model implementation. Chem Product Process Model 2015;10(3):147–59. https://doi.org/10.1515/cppm-2014-0031.
[45] Outi A, Rautavuoma I, van der Baan HS. Kinetics and mechanism of the Fischer-Tropsch hydrocarbon synthesis on a cobalt on alumina catalyst. Appl Catal 1981;1(5):247–72. https://doi.org/10.1016/0166-9834(81)80031-0. URL http://www.sciencedirect.com/science/article/pii/0166983481800310.
[46] Ostadi M, Rytter E, Hillestad M. Evaluation of kinetic models for Fischer-Tropsch cobalt catalysts in a plug flow reactor. Chem Eng Res Design 2016;114(Supplement C):236–46. https://doi.org/10.1016/j.cherd.2016.08.026. URL http://www.sciencedirect.com/science/article/pii/S0263876216302775.
[47] Weber A, Ivers-Tiffée E. Materials and concepts for solid oxide fuel cells (sofcs) in

stationary and mobile applications. J Power Sources 2004;127:273–83.
[48] Moran MJ, Shapiro HN, Boettner DD, Bailey MB. Fundamentals of engineering thermodynamics. John Wiley & Sons; 2010.
[49] Peters M, Timmerhaus K, West R. Plant design and economics for chemical engineers, civil engineering. McGraw-Hill Education; 2003. URL https://books.google.no/books?id=3uVFkBBHyP8C.
[50] Ulrich GD. Chemical engineering process design and economics: a practical guide. Process Publishing; 2004. URL https://books.google.no/books?id=27kvAAAACAAJ.
[51] Woods DR. Rules of thumb. Wiley-VCH Verlag GmbH & Co. KGaA; 2007. p. 1–44. https://doi.org/10.1002/9783527611119.ch1.
[52] Martelli E, Kreutz T, Carbo M, Consonni S, Jansen D. Shell coal IGCCS with carbon capture: conventional gas quench vs. innovative configurations. Appl. Energy 2011;88(11):3978–89. https://doi.org/10.1016/j.apenergy.2011.04.046.
[53] Larson ED, Jin H, Celik FE. Large-scale gasification-based coproduction of fuels and electricity from switchgrass. Biofuels, Bioprod Biorefin 2009;3(2):174–94. https://doi.org/10.1002/bbb.137.
[54] Trømborg E, Havskjold M, Lislebø O, Rørstad PK. Projecting demand and supply of forest biomass for heating in Norway. Energy Policy 2011;39(11):7049–58. https://doi.org/10.1016/j.enpol.2011.08.009.
[55] Anantharaman R, Bolland O, Booth N, van Dorst E, Ekstrom C, Sanchez Fernandes E. European best practice guidelines for assessment of $CO_2$ capture technologies, FP7-Energy, project 213206 CAESAR, 2011;1–112.
[56] Chen C, Rubin ES. $CO_2$ control technology effects on IGCC plant performance and cost. Energy Policy 2009;37(3):915–24. https://doi.org/10.1016/j.enpol.2008.09.093.
[57] Oil and petroleum products – a statistical overview. URL http://ec.europa.eu/eurostat/statistics-explained/index.php/Oil and petroleum products – a statistical overview.
[58] Ecb, Prices And Costs of EU Energy, European Central Bank Monthly Bulletin 2008;(3):58–65. URL http://search.proquest.com/docview/58772249?accountid=13042%5Cnhttp://oxfordsfx.hosted.exlibrisgroup.com/oxford?urlver=Z39.88-2004&rftvalfmt=info:ofi/fmt:kev:mtx:journal&genre=article&sid=ProQ:ProQ:pais&atitle=Prices+And+Costs&title=European+Central+Ba.
[59] Schmidt O, Gambhir A, Staffell I, Hawkes A, Nelson J, Few S. Future cost and performance of water electrolysis: an expert elicitation study. Int J Hydrogen Energy 2017;42(52):30470–92. https://doi.org/10.1016/j.ijhydene.2017.10.045.
[60] International Renewable Energy Agency (IRENA). Technology Roadmap, 2018. arXiv:arXiv:1011.1669v3, doi:10.1007/SpringerReference7300. URL http://www.solarpaces.org/wp-content/uploads/IRENA_2017_Power_Costs_2018.pdf%0Ahttp://www.springerreference.com/index/doi/10.1007/SpringerReference_7300.